

## Reviewed Preprint

v1 • July 10, 2026

Not revised

## ✉ For correspondence:

narottam\_acharya@ils.res.in

## Competing interests: No

competing interests declared

## Funding: See page 31

## Reviewing editor: Andrés Aguilera,

CABIMER, Universidad de Sevilla,

Spain

© 2026, Subhadarsini et al. This article is distributed under the terms of the [Creative Commons Attribution License](#), which permits unrestricted use and redistribution provided that the original author and source are credited.

# PCNA-Pol $\kappa$ -Pol $\delta$ /USP18 axes stabilize replication fork and restart to reduce cisplatin cytotoxicity

Ipsita Subhadarsini<sup>1,2</sup>, Jugal Kishor Sahu<sup>1,2</sup>, Shweta Thakur<sup>1</sup>, Rupesh Dash<sup>1</sup>, Narottam Acharya<sup>1</sup> ✉<sup>1</sup>Laboratory of Genomic Instability and Diseases, Department of Infectious Disease Biology, Institute of Life Sciences, Bhubaneswar, India • <sup>2</sup>Regional Center of Biotechnology, Faridabad, India

## eLife Assessment

Building on earlier studies, this manuscript reports a role for pol kappa in cisplatin resistance in the very specific scenarios of head and neck squamous cell carcinoma, providing evidence that the PIP box of Pol kappa is critical for cisplatin resistance in these cells. The findings are of a highly focused relevance and will be **useful** in the field, but the conclusions are limited to very specific cancer cells. Conclusions cannot be generalized to all cisplatin resistance mechanisms and cell types and are based on **incomplete** evidence that presents uncertainties and discrepancies that need to be resolved.

<https://doi.org/10.7554/eLife.112155.1.sa4>

## Abstract

Cisplatin and its analogues are valuable anti-cancer drugs that target the genome, block DNA replication, and induce apoptosis. As a counteractive response, cancer cells activate several mechanisms to maintain uninterrupted DNA replication, and those are yet to be fully elucidated. This study using head and neck squamous carcinoma cells (HNSCC) demonstrated the involvement of DNA polymerase Kappa (Pol $\kappa$ ), a trans-lesion DNA synthesis (TLS) polymerase that primarily functions as a mismatch extender, in cisplatin resistance. Interestingly, the catalytic activity of Pol $\kappa$  plays a minimal role in adduct bypass; rather, tripartite interactions involving it, rewire and stabilize the stalled replication fork. While the Pol $\kappa$ -PCNA-Pol $\delta$  axis facilitates efficient proliferation of cisplatin-resistant cells, the Pol $\kappa$ -PCNA-USP18 axis stabilizes critical proteins of ATM-ATR, and HR and NHEJ pathways to protect replication fork, repair damage, and restart DNA synthesis under cisplatin-induced stress. In resistant cells, the efficiency of ubiquitin-mediated proteasomal degradation is low, which is further diminished by Pol $\kappa$ -recruited USP18 deubiquitinase, maintaining a cellular homeostasis. In conclusion, for the first time, we uncovered two critical Pol $\kappa$  axes crucial for regulating cisplatin toxicity in cells and provided foundation for future drug discovery against advance HNSCC by targeting this non-essential DNA polymerase.

## Introduction

Cisplatin (cis-diamminedichloroplatinum (II)) is one of the widely used metal-based chemotherapeutic drugs to treat cancers like testicular, ovarian, bladder, lung, cervical, head and neck, gastric cancers, etc. (Dasari and Tchounwou 2014 [↗](#); Ghosh 2019 [↗](#)). Cisplatin exerts its anticancer activity by generating Pt-DNA adducts by cross-linking the N7 atoms of adjacent purines, preferably guanines of the same and different DNA strands, at several places of the nuclear and mitochondrial genome simultaneously. Thereby, the generated lesions block both DNA replication and transcription and activate several transduction pathways, which finally lead to apoptosis in rapidly proliferating tumor cells. The clinical success of cisplatin is compromised because of the development of intrinsic and acquired chemoresistance and dose-limiting cytotoxicity. Reduced efficacy of cisplatin depends on multiple factors, such as reduced drug

accumulation by efficient efflux pumps and sequestration by certain proteins, inactivation of the drug by binding with different proteins, success in inducing DNA damage, increase of cellular DNA repairing ability, activation of DNA damage tolerance pathways, and alteration of different proteins that signal to apoptosis (Maji et al. 2018).

Repair and bypass of cisplatin DNA adducts by nucleotide excision repair (NER) and by specialized DNA polymerases during translesion DNA synthesis (TLS), respectively, are key to cisplatin resistance (Duan et al. 2020). Studies reported that intrinsic low expression of NER proteins and low NER activity are the main reasons behind the impressive clinical success of cisplatin against metastatic testicular germ cell tumors (Masters and Koberle 2003; Welsh et al. 2004). Recent CRISPR-Cas9 based screening analysis suggested a role of transcription-coupled NER (TC-NER) in cisplatin resistance (Slyskova et al. 2018). Interstrand cisplatin cross-links are easily recognized and repaired by NER, whereas less efficient recognition of intrastrand cross-links leads to their higher abundance in the cells and therefore, they are highly cytotoxic (Sarkar et al. 2006). TLS is an alternative DNA replication process that enables bypass of DNA lesions encountered during DNA replication that usually cannot be performed by high fidelity replicative DNA polymerases Pol $\delta$  and Pol $\epsilon$ , and is emerging as a primary chemotherapeutic target (Acharya et al. 2020a). Not only TLS polymerases protect normal cells from cisplatin-induced genome instability during chemotherapy, but they also reduce the cisplatin toxicity in tumor cells by preventing the replication fork collapse and cell death, and thereby, they contribute to cisplatin resistance. Human cells harbor Y-family DNA polymerases like REV1, Pol $\eta$ , Pol $\iota$ , and Pol $\kappa$  that bypass specific DNA lesions (Acharya et al. 2020a). Among these, the role of Pol $\eta$  in bypassing Pt-GG lesions has been extensively studied both in yeast and human (Ummat et al. 2012; Zhao et al. 2012; Manohar et al. 2018). An increased expression of Pol $\eta$  has impacted cisplatin therapy and survival time of patients with non-small-cell lung cancer, ovarian cancer, and metastatic gastric adenocarcinoma (Chin et al. 2008; Srivastava et al. 2015).

Co-crystal structural analyses suggested that the catalytic pocket of Pol $\eta$  accommodates Pt-GG lesion without any steric hindrance and allows successful error-free bypass (Ummat et al. 2012; Zhao et al. 2012). Contrarily, an alternate Pol $\iota$ /Pol $\theta$ -dependent error-prone TLS pathway can replicate through cisplatin intrastrand cross-links. For both of these pathways, Rev1 is required as an indispensable scaffolding component of Pol $\eta$  and Pol $\iota$  (Lin et al. 2006; Yoon et al. 2015; Yoon et al. 2021). Although Pol $\zeta$ , a complex of Rev3 and Rev7, belongs to the B-family, it can participate in TLS (Baynton et al. 1998). While Pol $\zeta$  is not required for TLS opposite cisplatin-induced intrastrand cross-links in normal cells, studies suggested that cancer cells require Rev1-Pol $\zeta$ , and depletion of Rev1 or Rev3 sensitizes cancer cells to cisplatin, suggesting its role in chemoresistance (Doles et al. 2010; Zhu et al. 2016). Another study revealed that Pol $\eta$  contributes minimally in promoting TLS through cisplatin analogues like oxaliplatin, satraplatin, and picoplatin, whereas Rev1 and Pol $\zeta$  play a critical role in bypassing all four platinum analogs (Sharma et al. 2012). In contrast to other TLS Pols, the role of Pol $\kappa$  in lesion bypass remains poorly defined. Biochemical assays suggested that Pol $\kappa$  is mostly inefficient in inserting nucleotides opposite cisplatin-induced major groove DNA lesions; however, it can act as a mismatch extender to facilitate complete bypass (Haracska et al. 2002; Wolffe et al. 2003; Vasquez-Del Carpio et al. 2011; Jha and Ling 2018). Pol $\kappa$  can bypass the minor groove of DNA damages like benzo[a]pyrene and acylfuvenes (Ohashi et al. 2000; Ogi et al. 2002). A recent study reported that while bypassing minor groove DNA lesions, Pol $\kappa$  activity is dependent on PCNA ubiquitination but independent of Rev1, whereas TLS through major groove adducts and abasic sites, Pol $\kappa$  mostly plays a structural role and stabilizes the Rev1-Pol $\zeta$  extension complex on DNA, which is also regulated by ubiquitinated PCNA (Selles-Baiquet et al. 2025).

Uninterrupted DNA replication in cancer cells is a major driver of chemoresistance, as tumor cells often develop mechanisms to maintain replication fork progression despite the damage induced by chemotherapy, leading to treatment failure. Since we observed overexpression of Pol $\kappa$  in specific tumors upon cisplatin exposure, and among the TLS pols, its role in chemoresistance is least reported, this study established and explored underlying TLS and non-TLS mechanisms by which Pol $\kappa$  maintains DNA replication continuity to induce cisplatin chemoresistance. We

uncovered several axes by which Polk facilitates uninterrupted DNA replication in cancer cells to nullify cisplatin toxicity. We found that Polk rewires replication machinery specifically in cisplatin-resistant cancer cells by establishing a tripartite interaction with PCNA-Pol $\delta$  to enhance cellular proliferation. Polk maintains cellular homeostasis of several checkpoint and DDR proteins by preventing their ubiquitin-mediated proteasomal degradation by recruiting USP18 deubiquitinase. Finally, we propose that targeting Polk and USP18, the efficacy of cisplatin, the first-line cancer drug, can be improved.

## Results

### Polk is markedly upregulated in specific cancer cells upon cisplatin treatment and cisplatin-resistant oral squamous cell carcinoma (OSCC)

The expression of DNA polymerase involved in TLS of a specific lesion is usually get hyperregulated when the cells are exposed to the genotoxic agents that generate such lesions in the genome. To determine a possible role of Polk in cisplatin resistance, a panel of tumour specific cell lines from breast (MCF7 and MDA-MB-231), brain (SH-SY5Y), liver (Huh7), head and neck (H357 and SCC9), pancreatic (MIAPaCa-2), prostate (DU145) and lungs (A549) cancers along with a transformed but non-tumorigenic cell line HEK293 (Human embryonic kidney) were treated with 10  $\mu$ M of cisplatin for 24 hrs and the expression of Polk was determined by Western analysis (Figure 1A and B [↗](#)). Since the role of Pol $\eta$  in cisplatin chemoresistance has already been reported, we also checked its expression in these cells. We observed a tumour-specific hyperexpression of Pol $\eta$  and Polk upon cisplatin exposure. While in lung cancer and noncancerous HEK293 cells, the expression of Pol $\eta$  was increased by 2-3 folds upon cisplatin treatment in comparison to untreated controls, no significant change in expression was observed in other cell types. Polk was overexpressed in HNSCC cell lines when they were treated with cisplatin, but not in other tumour cells. Interestingly, the pancreatic cancerous cells showed overexpression of both Pol $\eta$  and Polk upon cisplatin exposure. This result suggested that cisplatin resistance in a particular tumour could be TLS DNA polymerase-specific.

To strengthen further, we checked and compared the expression of various DNA polymerases in cisplatin resistant H357 (H357-R) and SCC9 (SCC9-R) cells with those in sensitive parental isogenic cells (H357-S and SCC9-S). H357-R and SCC9-R cells have been used in several studies and these cells can tolerate up to 40  $\mu$ M of cisplatin, which is 3-4 folds more than the IC<sub>50</sub> values (10-15  $\mu$ M) (Mohapatra et al. 2021 [↗](#); Shriwas et al. 2021 [↗](#)). Briefly, these resistant cells were generated by chronic exposure of gradual increasing dose (upto IC<sub>50</sub>) of cisplatin over a period of 8 months and resistant cells were selected out (Figure 1C [↗](#)). Human cells possess 15 DNA polymerases that belong to A, B, X, and Y families (Acharya et al. 2020a [↗](#)). The expressions in terms of transcripts and protein levels of most of these Pols were checked by both reverse transcription PCR (RT-PCR) and Western analyses (Figure 1 D and E [↗](#), Supp. Figure 1A i and ii [↗](#)). p125 and Rev7 were checked as a subunit of Pol $\delta$  (p125-p50-p68-p12) and Pol $\zeta$  (Rev3-Rev7) holoenzyme complexes, respectively. In these cisplatin resistant cells, the transcript and protein levels of most of these polymerases did not alter significantly except Rev1 and Polk. To our surprise, notable polymerases like Pol $\eta$  and Pol $\zeta$  those were reported to be involved in cisplatin resistance in various cancer types, remained unaltered in resistant OSCC cells. Since Polk was highly dysregulated in resistant cells than Rev1, its role in chemoresistance was further explored in greater details.

### Polk depletion re-sensitizes resistant OSCC cells to cisplatin

To investigate how *POLK* deficiency would manifest in cisplatin sensitivity of resistant cancer cells, we decided to delete the gene using the CRISPR-Cas9 technique in H357-R and SCC9-R cells. While we were able to successfully generate and select *POLK*<sup>-/-</sup> clones of H357-R (H357-R *POLK* KO) as confirmed by Western blotting, despite our several attempts, we could not generate a similar clone in SCC9 (Supp. Figure 1B [↗](#) and Figure 2A-lanes 5 and 6 [↗](#)). Therefore, for subsequent

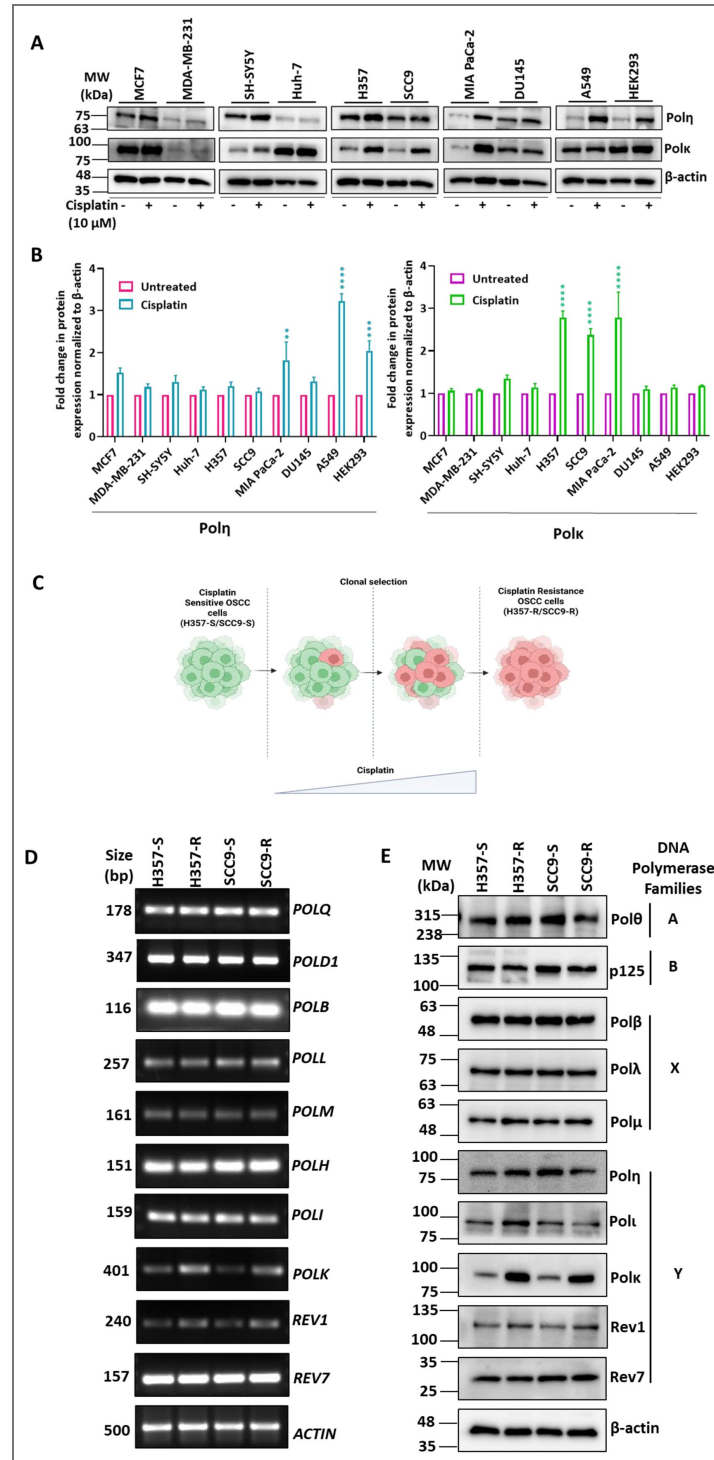


**Figure 1. Dysregulation of Polk in cisplatin treated and resistant cancer cells.**

(A) Western blot analyses of various cell-free lysates of cell lines without and treated with 10 μM cisplatin were carried out using Polη and Polk antibodies. β-actin was used as a loading control. (B) Protein band intensities were estimated and fold change after β-actin normalization was shown in bar graph as mean ± SEM (n=2). Statistical significance determined by two-way ANOVA, Šidák’s multiple comparisons test (\*\*p < 0.01, \*\*\*p < 0.001, \*\*\*\*p < 0.0001). (C) Schematic representation of generation of cisplatin resistant OSCC cell lines (H357-R and SCC9-R) from their respective cisplatin sensitive H357-S and SCC9-S cells. (D) RT-PCR analysis of various DNA polymerases in cisplatin resistant and sensitive OSCC cells. ACTIN was taken as a loading control. (E) Western blot analyses of lysates of OSCC cells using specific antibodies of various DNA polymerases or their subunits as mentioned. β-actin was detected as a loading control.

analyses, H357-R *POLK* KO cells were considered. When these cells were subjected to cisplatin treatment, an increased expression of Polk in H357-S by 2-3 folds in comparison to untreated was observed (Fig. 2A [↗](#), compare lane 1 with 2, Supp. Figure 1C [↗](#)). However, as shown earlier in this study, the Polk level was very high in H357-R without and with cisplatin exposure than in H357-S (compare lanes 3 and 4 with 1). This result was further confirmed by immunofluorescence analysis, where a higher amount of immune-stained Polk was observed in resistant than sensitive cells (Supp. Figure 1D i and ii [↗](#)). MTT-based and clonogenic cell survival assays revealed that while H357-R cells were resistant to cisplatin, both H357-S and H357-R *POLK* KO cells were hypersensitive, *albeit* more so in the Polk-deficient cells (Fig. 2B and C [↗](#)). IC50 values of H357-S and H357-R *POLK* KO cells were nearly 6-10 $\mu$ M, whereas for H357-R, it was estimated to be >32 $\mu$ M. Cell death due to cisplatin treatment by Annexin-V and PI staining FACS analyses further ascertained that the depletion of Polk re-sensitizes OSCC resistant cells to cisplatin, as a higher percentage of apoptotic cells was estimated in both H357-S and H357-R *POLK* KO cells upon cisplatin treatment (Fig. 2D i and ii [↗](#)). As expected, a higher percentage of the resistant H357-R cells still survived despite cisplatin treatment. Altogether, our results confirmed that the overexpressed Polk is responsible for inducing cisplatin chemoresistance in H357 OSCC cells.

## Polk depletion enhances genomic instability and delays cell cycle progression in resistant OSCC cells

Since Polk is a TLS polymerase, its absence can cause accumulation of damaged DNA due to cisplatin adducts associated with replication fork collapse. Therefore, to correlate cellular sensitivity with DNA damage accumulation in Polk depleted cells, DNA damage status in these cells due to cisplatin treatment was determined. The comet assay confirmed increased DNA tailing of genomic DNA in Polk-depleted cells following cisplatin treatment, indicating a higher percentage of DNA degradation. While minimal tailing was observed in H357-R cells, H357-S cells also showed DNA tailing when exposed to sub-optimal concentrations of cisplatin (Figure 3A i and ii [↗](#)). To further confirm the re-sensitization of H357-R cells to cisplatin due to the lack of Polk, other DNA damage markers like  $\gamma$ H2A.X ( $\gamma$ H2A.X) and cleaved PARP1 were checked.  $\gamma$ H2A.X is a sensitive biomarker for the presence of DNA double-strand breaks (DSBs). After a DSB occurs, ATM and DNA-PK phosphorylate the serine-139 residue of histone variant H2A.X, forming  $\gamma$ H2A.X foci that act as “anchors” to recruit DNA repair proteins to the site of damage (Mah et al. 2010 [↗](#)). Both immunofluorescence and Western analyses suggested that a higher percentage of  $\gamma$ H2A.X foci as a cellular response to DNA damage in H357-S and H357-R *POLK* KO than in H357-R cells upon cisplatin treatment (Figure 3B i and ii [↗](#), Figure 3C [↗](#), and Supp. Figure 2A [↗](#)). The phosphorylation of H2A.X to  $\gamma$ H2A.X creates binding sites that enhance PARP1's affinity and its catalytic efficiency, thereby stabilizing PARP1 at the damage site and facilitating DNA repair. However, in excessive DNA damage conditions, the cell may initiate apoptotic pathways, leading to PARP1 cleavage by activated caspases, producing 89 kDa and 55 kDa fragments (Kumari et al. 2025 [↗](#)). We observed more accumulation of cleaved PARP1 when H357-S and H357-R *POLK* KO cells were treated with cisplatin (Figure 3D [↗](#), Supp. Figure 2B [↗](#)). Despite cisplatin treatment, H357-R cells did not show any increase in  $\gamma$ H2A.X foci and PARP1 cleavage, suggesting efficient repair of DNA breaks. Notably, cleaved PARP1 product was observed even in untreated H357-R *POLK* KO cells. These results indicated that due to lack of Polk, cells can accumulate DSBs in the presence of cisplatin drug. In that context, Polk depletion may affect cell cycle progression. Therefore, a synchronized population of various cells post a double-thymidine block was allowed to proliferate without and with 5  $\mu$ M cisplatin, and cells were harvested and analyzed by FACS (Figure 3E i and ii [↗](#), Supp. Figure 2C i and ii [↗](#)). Without cisplatin, while both H357-S and H357-R cells progressed through a complete cell cycle within 12 hrs, we observed a significant delay in the progression of Polk-depleted cells, as the majority of the cells were stuck in the G2/M phase (9-12 hours). This observation also corroborates with more  $\gamma$ H2A.X foci and cleaved PARP1 accumulation in H357-R *POLK* KO cells, which were further heightened upon cisplatin treatment. Chronic exposure to cisplatin significantly delayed the progression of cell cycles of H357-S and H357-R *POLK* KO cells compared to H357-R cells. At 6 hrs, most of the cells of H357-S and H357-R *POLK* KO were still in G1/S phase, while H357-R cells were accumulated in G2/M phase (Supp. Figure 2C [↗](#)). Since the cell

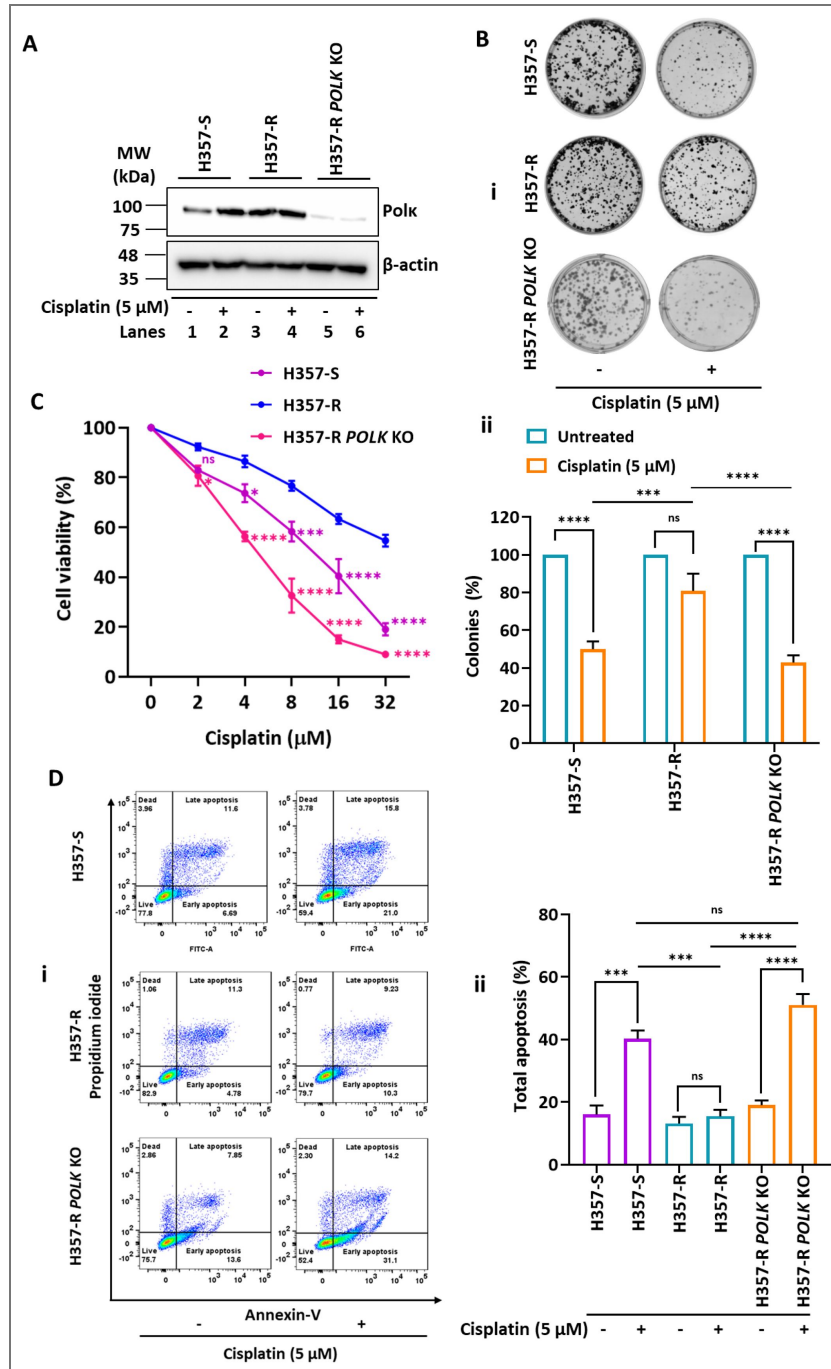


**Figure 2. Absence of Polk re-sensitizes OSCC resistant cells to cisplatin.**

(A) H357-S, H357-R and H357-R POLK KO cells were treated with 5 μM cisplatin and analyzed for Polk expression by Western blot analysis. β-actin was used as a loading control. (B) Colony-forming assay was performed using H357-S, H357-R and POLK KO cells without and with 5 μM cisplatin (i). Bar graph represents colony percentage as mean ± SEM (n=3) as determined by two-way ANOVA with Tukey's multiple comparisons test (\*\*\*p < 0.001, \*\*\*\*p < 0.0001, and ns- nonsignificant) (ii). (C) Cells were treated with cisplatin for 48 hours and then MTT assays were performed. Graph indicates the mean ± SEM (n=3), two-way ANOVA with Tukey's multiple comparisons test (\*p < 0.05, \*\*p < 0.001, \*\*\*\*p < 0.0001, and ns- nonsignificant). Purple asterisks indicate comparison between H357-R to H357-S, pink asterisks indicate comparison between H357-R to H357-R POLK KO. (D) After treatment with 5 μM cisplatin for 48 hours, cells were stained with Annexin V/PI and analyzed by flow cytometry. Percentage of cells in each quadrant is as indicated (i). Bar graph represents percentage of total apoptosis (early and late apoptosis). Data were represented as mean ± SEM (n=3). Statistical significance determined by two-way ANOVA, Tukey's multiple comparisons test, (\*\*\*p < 0.001, \*\*\*\*p < 0.0001, and ns- nonsignificant) (ii).

cycle progression was affected upon Polk depletion even without genotoxic stress, we wanted to check cellular proliferation by measuring Ki-67 expression. A higher percentage of Ki-67 positive cells usually indicates increased cellular proliferation, and the immunofluorescence assay suggested a higher percentage of Ki-67 positive resistant OSCC cells (85-95%), which reduced significantly upon Polk depletion (Supp. Figure 2D i and ii [↗](#)). It suggests that Polk contributes to the proliferative capacity of H357-R cells. Altogether, these data suggested that Polk's function is associated with multiple phenotypes of resistant OSCC cells as its absence accumulates DNA breaks, induces apoptosis, delays cell cycle progression, and cellular proliferation without and with cisplatin exposure. Thus, Polk plays a crucial role in stabilizing and recovering replication fork post-cisplatin-induced DNA damage and probably also the replication of undamaged DNA of H357-R cells.

## Rewiring of DNA replication in cisplatin-resistant OSCC cells by DNA polymerase Kappa

Since we observed a lesser colonization efficiency, reduced proliferation rate, and a slower cell cycle progression of *POLK* depleted H357-R cells under normal physiological conditions, we hypothesized that DNA replication in these cells might have been rewired to be Polk dependent. To test further, sensitivity of various OSCC cells to replication inhibitors was determined (Figure 4A [↗](#)). While hydroxyurea (HU) depletes the cellular level of dNTPs, aphidicolin inhibits DNA synthesis by binding near the dNTP-binding site of replicative DNA polymerases like Pol $\delta$ . Camptothecin (CPT) works by inhibiting DNA Topoisomerase I, an enzyme crucial for DNA replication. We found that H357-S and H357-R *POLK* KO exhibited a higher lethality to these drugs than H357-R cells, and interestingly, cells lacking Polk showed the maximal sensitivity, indicating an unexpected role of a TLS Pol during normal DNA replication. Since the processive DNA synthesis during replication in human cells is mostly coordinated by Pols  $\delta$  and  $\epsilon$ , it is intriguing to determine whether Polk plays a structural or catalytic role and if its interaction with PCNA becomes important in such an event. In our earlier study, we identified two PIP motifs (528-SIIGFL-533 and 864-TLDIFF-869) in Polk required for PCNA binding, and showed that TLS occurs normally in human fibroblast cells in which the *pip1* or *pip2* mutant Polk is expressed, but mutational inactivation of both PIPs rendered Polk nonfunctional in TLS (Yoon et al. 2014 [↗](#)). To delineate the importance of the catalytic domain and PIP motifs of Polk in DNA replication of OSCC cells, WT, catalytically dead (D198A, E199A), and PIP mutant (F532A, L533A, F868A, F869A) of Polk were transfected into H357-R *POLK* KO cells and the susceptibility of the transfectants to replication inhibitors was determined (Figure 4B and C [↗](#)). By probing with anti-GFP antibody, first we confirmed that all the transfectants were equally expressing Polk, but not in the vector control (Figure 4B [↗](#)). The cytotoxicity assays in the presence of HU, Aphidicolin, and CPT revealed that the overexpression of the wild type and catalytically dead mutants of Polk could suppress the sensitivity of H357-R *POLK* KO cells, but not by overexpressing the PIP mutant, and its sensitivity remained the same with the cells harboring vector control (Figure 4C [↗](#)). These results suggested that Polk plays mostly a structural role and allows DNA synthesis by the replicative polymerase efficiently, however, its interaction with PCNA becomes important. To demonstrate a direct role of Polk in DNA replication, DNA fiber assay was conducted as depicted in the ray diagram (Figure 4D [↗](#)). In this assay, cells are allowed to incorporate nucleotide analogs into nascent DNA during replication, which can be detected by immunostaining, and it allows real-time monitoring of several replication parameters, such as speed, stalling, and origin firing at single-molecule resolution. CldU incorporation into DNA before HU treatment and IdU incorporation during replication restart were followed, and about 300 DNA fibers were monitored (Supp. Table-1 [↗](#)). The replication velocity of H357-R ( $\sim 0.159 \mu\text{m}/\text{min}$ ) was almost double that of H357-S and H357-R *POLK* KO cells ( $\sim 0.08 \mu\text{m}/\text{min}$ ) (Supp. Table-1a [↗](#)). Although the firing of new origins in these cells was unaffected ( $\sim 10\%$ ), a higher percentage of stalled/collapsed forks was detected in H357-S and H357-R *POLK* KO cells ( $\sim 30\%$ ). Interestingly, the percentage of fork restart was relatively higher in H357-R cells ( $\sim 70\%$ ), suggesting that the replication recovery from replication stress due to HU is more efficiently performed if a cell has abundant Polk (Supp. Table-1b [↗](#)). Next, to determine any physical contacts between Polk and replicative Pols on PCNA that facilitates efficient replication

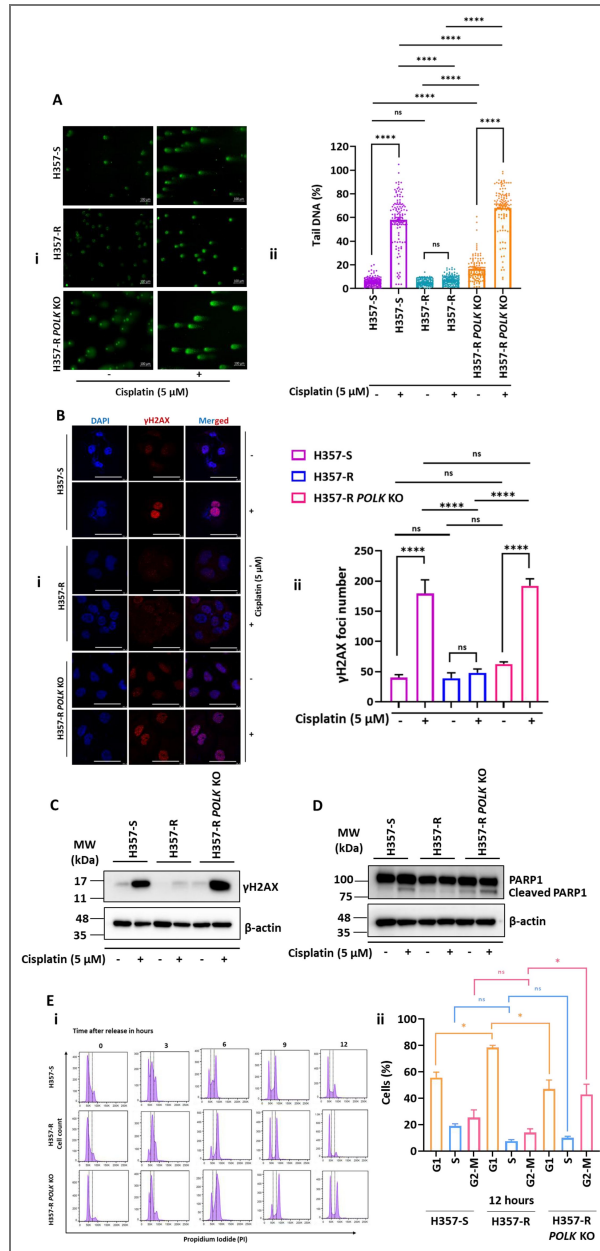


**Figure 3. Absence of Polk enhances genomic instability and delays cell cycle progression in OSCC resistant cells.**

**(A)** Representative alkaline comet images showing DNA tailing in cells following treatment with 5 μM of cisplatin for 48 hours **(i)**. The bar graph represents percentage of tail DNA. Data represented as (mean ± SEM; n=3). Statistical significance determined by two-way ANOVA with Tukey's multiple comparisons test (\*\*\*\*p < 0.0001, and ns- nonsignificant) **(ii)**. **(B)** Representative immunofluorescence images of H357-S, H357-R and H357-R *POLK* KO cells showing γH2AX (red) puncta and DAPI (blue) and corresponding merged images **(i)**. Quantification of γH2AX foci numbers is indicated in a bar diagram as mean ± SEM (n=3) **(ii)**. Statistical significance determined by Ordinary one-way ANOVA, Tukey's multiple comparisons test, (\*\*\*\*p < 0.0001, and ns- nonsignificant). Scale bars indicate 7.5 μm. **(C)** Western blot analyses of H357-S, H357-R and H357-R *POLK* KO lysate using γH2AX antibody was carried out. β-actin was used as a loading control. **(D)** Western blot analyses of H357-S, H357-R and H357-R *POLK* KO lysate probed with PARP1 antibody was carried out. β-actin was used as a loading control. **(E)** A representative cell cycle profiles of H357-S, H357-R and H357-R *POLK* KO cells at different time points after releasing from double-thymidine block were shown. G1, S, and G2M phases were demarcated **(i)**. The percentage of cells in G1, S and G2-M phases at 12 h is estimated and plotted. Data was represented as mean ± SEM (n=2) **(ii)**. Statistical significance determined by Ordinary one-way ANOVA, Tukey's multiple comparisons test, (\*p < 0.05, and ns- nonsignificant) **(ii)**.

and cellular proliferation, binding between Polk with Pol $\delta$  subunits was checked by immunofluorescence and immunoprecipitation. Human Pol $\delta$  consists of p125, the catalytic, and p50, p68, and p12 accessory subunits (Khandagale et al. 2019 [↗](#); Sahu et al. 2026 [↗](#)). Based on the compatibility of available antibodies, the nuclear localization of Polk with p50 and p12 subunits was conducted. We observed a higher population of co-localized nuclear puncta of Polk with p50, and Polk with p12 proteins in H357-R than in H357-S cells (Figure 4E [↗](#)). Further, these interactions were confirmed by co-immunoprecipitation in two ways (Figure 4F i and ii [↗](#)). The cellular extract was either precipitated by anti-Polk or anti-PCNA, and Pol $\delta$  subunits and other proteins were detected by respective antibodies. In both approaches, we observed interaction between Polk and Pol $\delta$  subunits, and both are bound to PCNA as well. Immunoprecipitation with IgG beads did not pull down any proteins. In a similar assay, no co-localization foci and interaction of Polk with a non-replicative polymerase Pol $\theta$  was observed (Supp. Fig. 3 [↗](#)). Altogether, these results suggested that Polk can participate in normal DNA replication in addition to its role as a TLS polymerase by coordinating with replicative DNA polymerases like Pol $\delta$ . For such a function, the catalytic domain of Polk becomes dispensable, whereas its interaction with PCNA is sufficient to drive efficient replication. This data established a key tripartite interaction of PCNA-Polk-Pol $\delta$  that facilitates efficient replication of OSCC-R cells.

## Catalytic independent function of Polk is required to protect the replication fork and restart post-cisplatin exposure

Since Polk depletion sensitized the H357-R cells to cisplatin, we argued that TLS activity by this DNA polymerase could be critical. Although there is no biochemical evidence to suggest insertion of nucleotides against cisplatin adducts by Polk, the catalytic activity may be required during the mismatch extension step during a two-DNA polymerase-based TLS, where one inserts and Polk extends (Wolfe et al. 2003 [↗](#)). In addition, to function during TLS, DNA polymerase kappa also has to interact with PCNA (Acharya et al. 2020b [↗](#)). To delineate the importance of catalytic domain and PIP motifs of Polk in cisplatin resistance of OSCC, after confirming about equal expression, the susceptibility of H357-R *POLK* KO cells harboring WT, catalytically dead (Polk CD: D198A, E199A), and PIP mutant (F532A, L533A, F868A, F869A) of Polk to cisplatin was determined (Figure 5A i [↗](#)). Colonogenic assay confirmed that while the wild type and catalytically inactive mutant Polk expressing cells (H357-R, H357-R *POLK* KO + GFP-Polk, and H357-R *POLK* KO + GFP-Polk CD) grew well and formed almost similar number of colonies without and with the presence of cisplatin again confirming the involvement of Polk in cisplatin resistance, to our surprise, the cells expressing PIP mutant of Polk formed significantly less number of colonies similar to the vector control and those numbers further reduced in the presence of cisplatin (Figure 5A [↗](#) ii and iii). MTT assay further confirmed that the ectopic expression of wild type and catalytically inactive mutant of Polk reduced sensitivity to cisplatin, and the viability in the presence of cisplatin decreases when the cells do not harbor (EV) or only express the PIP mutant (Figure 5B [↗](#)). To demonstrate a direct role of Polk in replication fork protection and restart upon cisplatin exposure, DNA fiber analysis was carried out. Replication was first blocked with cisplatin, and after washings, cells were allowed to replicate; and the DNA fibers were sequentially labelled with two thymidine analogues, detected by immunostaining, and analyzed (Figure 5C [↗](#), Supp. Table -2 a and b [↗](#)). While the replication fork speed of H357-R cells did not alter significantly without and with cisplatin treatment ( $\sim 0.3$   $\mu\text{m}/\text{min}$ ), in the case of H357-S and H357-R *POLK* KO cells, the fork speeds were much lower ( $\sim 0.25$ - $0.29$   $\mu\text{m}/\text{min}$ ) and further reduced under cisplatin stress ( $\sim 0.26$ - $0.22$   $\mu\text{m}/\text{min}$ ). Consequently, the percentage of stalled/collapsed replication forks (35%) was higher in H357-S and H357-R *POLK* KO cells than that in H357-R cells ( $\sim 15$ - $24\%$ ). Evidently, more actively replicating forks ( $\sim 66$ - $71\%$ ) were found in H357-R cells. The replication defects in the absence and presence of cisplatin in H357-R *POLK* KO cells were rescued by overexpressing catalytically active as well as inactive mutants of Polk (H357-R *POLK* KO + GFP-Polk, and H357-R *POLK* KO + GFP-Polk D198A, E199A), but not by the PIP mutant (H357-R *POLK* KO + GFP-Polk pip) (Figure 5D [↗](#) and Supp. Table - 3 [↗](#)). These results suggested Polk induces cisplatin resistance in H357 in a catalytically independent manner, but its interaction with PCNA is critical in protecting the replication fork and recovering thereafter. Moreover, the DNA fiber assay without cisplatin

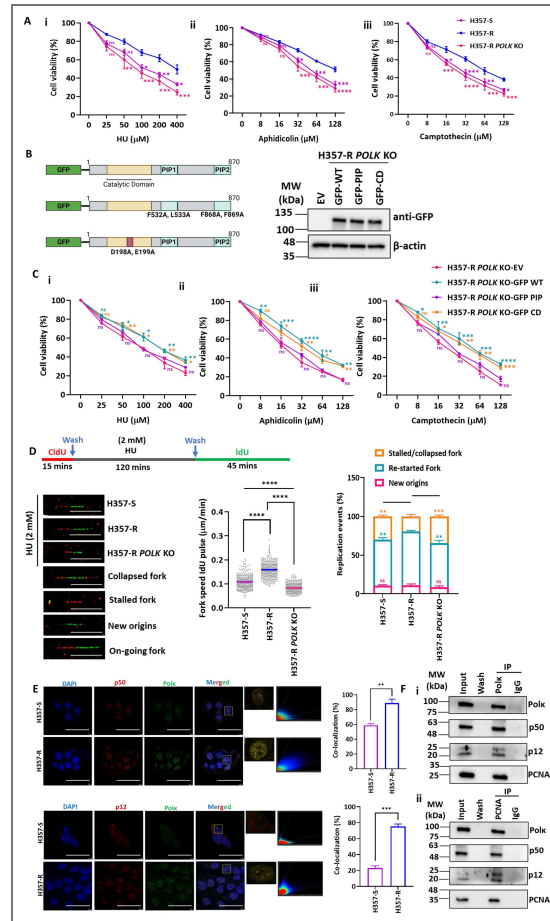


**Figure 4. DNA replication in OSCC cisplatin resistant cells is governed by Polk.**

(A) H357-S, H357-R and H357-R *POLK* KO cells were treated with the indicated concentration of drugs HU (i), Aphidicolin (ii) and Camptothecin (iii) for 24 hours, and then an MTT assay was performed. These graphs indicate the mean  $\pm$  SEM (n=3) and were analyzed by two-way ANOVA with Tukey's multiple comparisons test (\*p < 0.05, \*\*p < 0.01, \*\*\*p < 0.001, \*\*\*\*p < 0.0001, and ns- nonsignificant). Purple asterisks indicate comparison between H357-R to H357-S, pink asterisks indicate comparison between H357-R to H357-R *POLK* KO. (B) A schematic representation of the critical motifs of Polk and their mutations involved in catalytic activity and PCNA interaction is shown. Knockout cells harboring GFP-tag of WT, PIP mutant and Catalytically Dead (CD) Polk were analyzed by Western blotting. EV indicates cells possessing an empty vector.  $\beta$ -actin was taken as an internal control. (C) Transfected cells were treated with the indicated concentrations of HU (i), Aphidicolin (ii) and Camptothecin (iii) for 24 hours, and then MTT assays were performed. These graphs indicate the mean  $\pm$  SEM (n=2) and statistically verified by two-way ANOVA with Tukey's multiple comparisons test (\*p < 0.05, \*\*p < 0.01, \*\*\*p < 0.001, \*\*\*\*p < 0.0001, and ns-nonsignificant). Cyan, orange and violet asterisks indicate comparison between EV to GFP-WT, GFP-CD and GFP-PIP respectively. (D) A schematic representation of DNA fiber analysis in the presence of HU and representative images of various replication events in H357-S, H357-R and H357-R *POLK* KO cells were shown. The fork speeds were measured and the values of three independent experiments were pooled and plotted. Bar graph showing percentage of various replication events in H357-S, H357-R and H357-R *POLK* KO cells. Data were represented as mean  $\pm$  SEM (n=3). Statistical significance was determined by two-way ANOVA with Tukey's multiple comparisons test (\*\*p < 0.01, \*\*\*p < 0.001, \*\*\*\*p < 0.0001, and ns-non significant). Scale bars indicate 10  $\mu$ m. (E) Immunofluorescence co-localization analysis of H357-S and H357-R cells showing p12 and p50 subunits of Pol $\delta$  (red), Polk (green), DAPI (blue), and corresponding merged images. Merged images represent co-localization of Pol $\delta$  with Polk in the nucleus. Zoom-in merged (only green and red) view of dashed box area showed in upper right corner of corresponding image. Scatter plot of representative merged images is shown. Percentage of co-localization was shown in bar diagram. Scatter plot and co-localization percentage were obtained from confocal microscope Stellaris 5. Data were represented as mean  $\pm$  SEM (n=3). Statistical significance was determined by t-test, (\*\*p < 0.01, \*\*\*p < 0.001). Scale bars indicate 7.5  $\mu$ m. (F) Co-immunoprecipitation was performed in H357-R whole cell extract using either Polk or PCNA antibody. Interaction between Polk with PCNA/p50/p12/Polk and interaction between PCNA with Polk/p50/p12/PCNA were analyzed by Western blotting. IgG was considered as a negative control. Representative best immunoblots from two independent experiments are shown.

further confirmed that the replication defects in H357-R *POLK* KO cells are solely due to the loss of Polk, which can be rescued by a catalytically dead mutant of Polk. Thus, the non-TLS function of Polk plays an important role in the replication of both undamaged and cisplatin adducts containing the genome to endure uninterrupted DNA replication in chemoresistant OSCC.

## Polk depletion impairs ATM -ATR signaling and DNA strand break repair pathways

To delineate the underlying mechanisms by which Polk non-catalytically protects the genome from cisplatin damage, we were intrigued to explore various DDR pathways other than TLS. The ATM and ATR pathways are central to DNA damage response (DDR) that protect genomic integrity by sensing DNA damage, coordinating cell cycle checkpoints, and activating DNA repair mechanisms. While ATM is primarily activated by DSBs to activate downstream kinase Chk2, ATR responds to a broader range of DNA damage, including stalled replication forks, to activate Chk1 to execute the appropriate DNA repair pathways for cell survival, and failing to do so can lead to apoptosis (Casper et al. 2002 [↗](#); Hirao et al. 2002 [↗](#)). We found that the protein levels of ATM, ATR, and their phosphorylated forms were remained unaltered in all of these cells H357-S, H357-R and H357-R *POLK* KO without and with cisplatin treatment (Figure 6A [↗](#) and Supp. Fig. 4A [↗](#)). However, barely any Chk1 and Chk2 proteins were expressed in Polk depleted cells, accordingly no activated forms of these proteins (p-Chk1 and p-Chk2) were detected upon cisplatin damage (Figure 6A [↗](#) and Supp. Fig. 4A [↗](#)). Whereas a higher expression of p-Chk1 and p-Chk2 were detected in H357-S and H357-R with cisplatin treatment in comparison to untreated cells. This result indicated that activated ATM-ATR kinases can transduce DDR response in Polk-proficient cells, but failed to do so in Polk-deficient cells. ATM-Chk2 regulates DSB repair by homologous recombination (HR) and non-homologous end joining (NHEJ) pathways (Kumari et al. 2025 [↗](#)). Mre11-Rad50-Nbs1 (MRN) complex, upon binding to broken DNA, recruits and activates the ATM-Chk2 pathway. Further, they recruit CtIP to DSBs and phosphorylate it to facilitate resection. Chk2 activation leads to BRCA1 phosphorylation, aiding in the recruitment of Rad51 to DNA double-strand breaks. This action facilitates the correct assembly of the Rad51-BRCA2-ssDNA complex to carry out the error-free HR repair pathway. RAD54 helps the Rad51-coated DNA search for a homologous template sequence, a critical step for strand invasion. While HR is mostly an error-free repair pathway occurring in S phase, NHEJ is an intrinsically error-prone repair pathway occurring at all cell cycle stages. ATM phosphorylates core NHEJ factors such as DNA-PKCs, Artemis, XRCC4, and XLF, and DNA polymerase  $\lambda$  (Pol $\lambda$ ), generally promoting NHEJ. We checked the status of HR and NHEJ proteins in these cells (Figure 6B and C [↗](#)). We observed that while the MRN complex seems to be operational, the downstream proteins of HR are mostly missing only in H357-R *POLK* KO cells without and with cisplatin treatment (Figure 6B [↗](#) and Supp. Fig. 4B [↗](#)). Similarly, NHEJ pathway is also affected as some of the key downstream effectors like phospho-DNA-PKCs, Artemis, and DNA ligase IV were hardly detected in cisplatin treated H357-R *POLK* KO cells (Figure 6C [↗](#) and Supp. Fig. 4C [↗](#)). Again, the upstream factors of NHEJ pathway like Ku70-Ku80 heterodimer complex seems to be active in these cells. We reconfirmed these observations by taking nuclear fractions and Western analyses with specific antibody (Figure 6D [↗](#) and Supp. Fig. 4D [↗](#)). Nuclear localization analyses of these proteins by immunostaining further strengthened the observations (Supp. Fig. 5 [↗](#)). Altogether, these results suggested that Polk somehow regulate stabilization of downstream factors of cell cycle checkpoints, HR and NHEJ repair pathways to stabilize the replication fork and the genome.

## Polk dependent conserved pathways are involved in cisplatin resistance of SCC9 cells

To further strengthen our observations, we used another OSCC cell line, SCC9, to demonstrate the role of Polk in cisplatin resistance. Since we could not select *POLK*<sup>-/-</sup> clonal cells by using the CRISPR-Cas9 approach, we decided to use the siRNA approach to knock down *POLK* and characterize such cells further (Supp. Fig. 6 [↗](#)). First, we confirmed the efficacy of *POLK* siRNA, and it is able to knock down most of the transcripts, as we hardly detected any Polk protein by

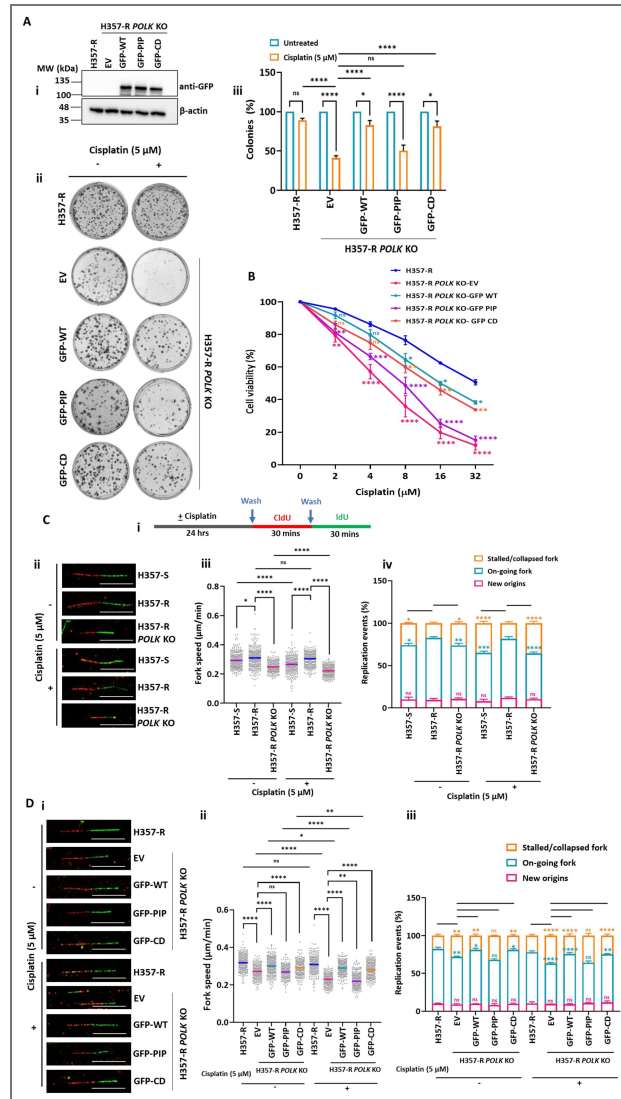


**Figure 5. Structural function of Polk in the protection replication fork and restart post-cisplatin exposure.**

**(A)** Western blot analysis shows ectopic expression of GFP-tagged WT, PIP mutant and Catalytically Dead (CD) mutants in H357-R *POLK* KO cells. EV indicates an empty vector.  $\beta$ -actin was considered as an internal control **(i)**. Colony-forming assay was performed using H357-R and H357-R *POLK* KO transfected cells **(ii)**. Bar graph represents colony percentage as mean  $\pm$  SEM (n=4), statistical significance was determined by two-way ANOVA with Tukey's multiple comparisons test (\* $p$  < 0.05, \*\*\*\* $p$  < 0.0001, and ns- nonsignificant) **(iii)**. **(B)** Cells were treated with the indicated concentrations of cisplatin for 48 hours and then an MTT assay was performed. These graphs indicate the mean  $\pm$  SEM (n=3), two-way ANOVA, Tukey's multiple comparisons test (\* $p$  < 0.05, \*\* $p$  < 0.01, \*\*\* $p$  < 0.001, \*\*\*\* $p$  < 0.0001, and ns- nonsignificant). Pink asterisks indicate comparison between H357-R to H357-R *POLK* KO EV. Cyan, orange and violet asterisks indicate comparison between EV to GFP-WT, GFP-CD and GFP-PIP respectively. **(C)** Schematic representation of DNA fiber analysis as carried out in the presence and absence of cisplatin **(i)**. Representative replication event images were shown **(ii)**. The fork speed were measured and the values of three independent experiments were pooled and plotted **(iii)**. Bar graph showing percentage of various replication events in H357-S, H357-R and H357-R *POLK* KO cells with and without cisplatin **(iv)**. Data were represented as mean  $\pm$  SEM (n=3). Statistical significance was determined by two-way ANOVA with Tukey's multiple comparisons test (\* $p$  < 0.05, \*\* $p$  < 0.01, \*\*\* $p$  < 0.001, \*\*\*\* $p$  < 0.0001, and ns-non significant). Scale bars indicate 10  $\mu$ m. **(D)** Representative images of DNA fibers in H357-R and H357-R *POLK* KO cells transfected with EV and mutants (GFP-WT, GFP-PIP, GFP-CD) without or with treatment with 5  $\mu$ M cisplatin for 24 hours before labelling are shown **(i)**. The fork speeds were measured and the values of three independent experiments were pooled and plotted for H357-R and H357-R *POLK* KO transfected cells with or without cisplatin **(ii)**. Bar graph shows the percentage of various replication events with and without cisplatin. Data were represented as mean  $\pm$  SEM (n=3) **(iii)**. Statistical significance was determined by two-way ANOVA with Tukey's multiple comparisons test (\* $p$  < 0.05, \*\* $p$  < 0.01, \*\*\*\* $p$  < 0.0001, and ns-non significant). Scale bars indicate 10  $\mu$ m.

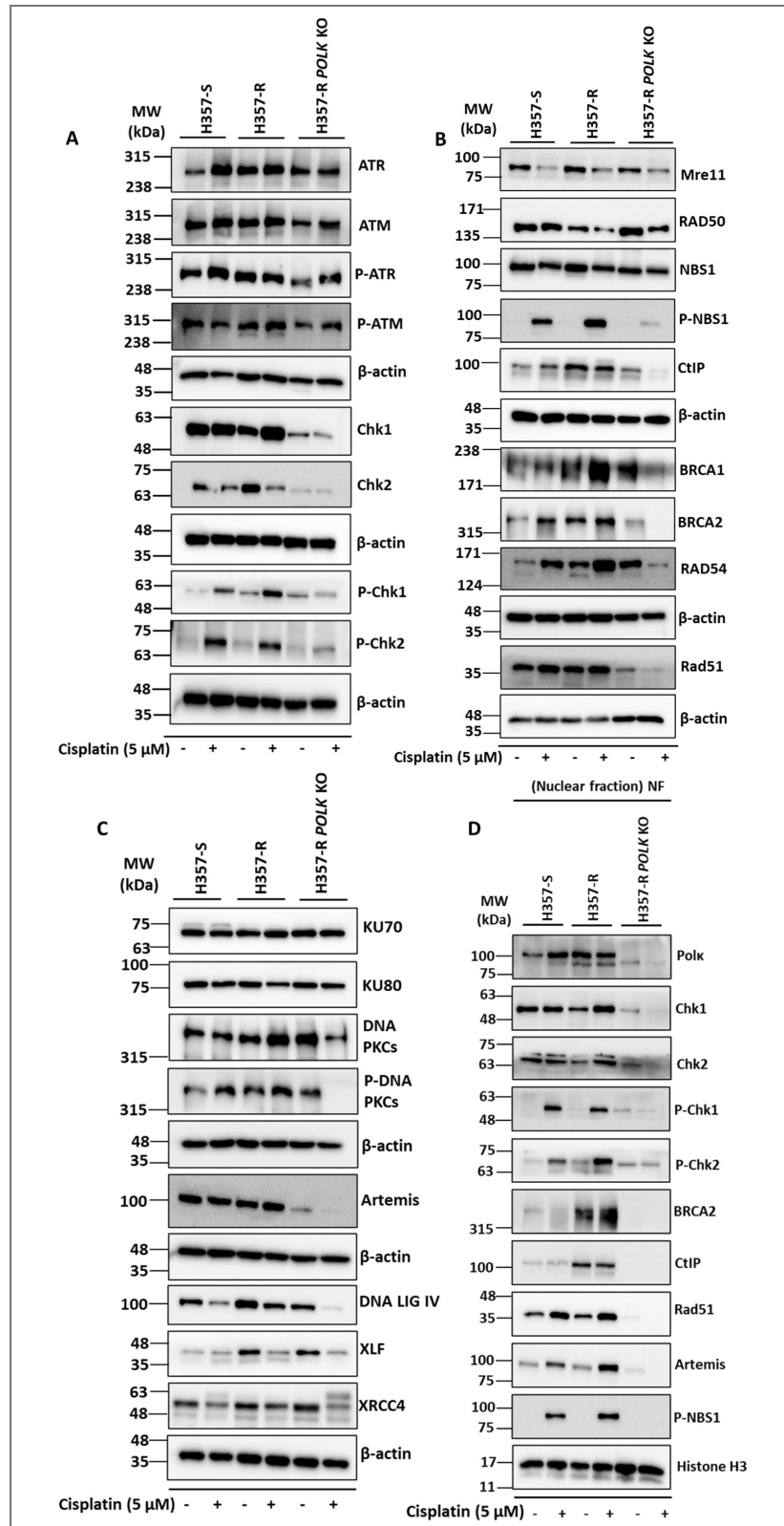


**Figure 6. Absence of Polk dysregulate ATM -ATR signaling and DNA strand break repair pathways.**

(A) Western blot analyses of cell-free lysates of H357-S, H357-R and H357-R *POLK* KO cells without and treated with 5  $\mu$ M cisplatin were carried out, and were probed with the indicated antibodies against checkpoint protein.  $\beta$ -actin was detected as a loading control. (B) Similar Western blot analyses but probed with antibodies of proteins involved in HR pathway. (C) Similar Western blot analyses but probed with antibodies of proteins involved in NHEJ pathway. (D) Western blot analyses of nuclear extracts of H357-S, H357-R and H357-R *POLK* KO cell lines without and treated with 5  $\mu$ M cisplatin were carried out and were probed with indicated specific antibodies. Histone H3 was used as a loading control.

Western and immunofluorescence analyses (Supp. Fig. 6A i [↗](#) and Supp. Fig. 6B [↗](#)). Cell viability assay suggested that the depletion of Polk re-sensitizes SCC9-R resistant cells to cisplatin and the IC50 value reduced from ~32  $\mu$ M to ~8  $\mu$ M of cisplatin (Supp. Fig. 6D [↗](#)). Comet assay,  $\gamma$ -H2A.X, and cleaved PARP1 detection further ascertained the role of Polk in protecting genome of SCC9 from damages caused by cisplatin (Supp. Fig. 6 C, E [↗](#), and Supp. Fig. 6A ii and iii [↗](#)). Absence of Chk1, Chk2, p-Chk1, p-Chk2, CtIP, BRCA2, Rad51, and Artemis in *POLK* knockdown SCC9 cells without and with cisplatin treatment suggested the possible critical role of Polk in activating and transducing cell cycle checkpoints to regulate HR and NHEJ to stabilize the genome (Supp. Fig. 6A iv-xi [↗](#)). This data confirmed that Polk plays conserved roles in inducing cisplatin chemoresistance, probably in all OSCC cells.

## Polk protects key checkpoint and DSB repair proteins from ubiquitin-mediated degradation

A low-level detection of some of the critical proteins of checkpoints and DDR pathways in the Polk-depleted cells could be due to a defect at the level of gene expression or at the post-translational event. Therefore, RNA expression in terms of cDNA was checked by agarose gel electrophoresis (Figure 7A i and ii [↗](#)). We observed cDNAs of transcripts encoded by *CHEK1*, *CHEK2*, *BRCA2*, *CTIP*, *RAD51*, and *ARTEMIS* genes in both Polk proficient and deficient H357-R cells, whereas, as expected, no cDNA was detected for *POLK* only in H357-R *POLK* KO cells. Next, we checked the expression of these proteins in the presence of MG132, an inhibitor that blocks the proteolytic activity of the 26S proteasome involved in the degradation of unneeded or damaged proteins. Our analyses suggested that MG132 has no effect on the protein levels in H357-R cells, whereas Chk1, Chk2, BRCA2, CtIP, Rad51, and Artemis proteins were recovered in H357-R *POLK* KO cells upon MG132 treatment, and barely any of these proteins were detected without the proteasomal inhibitor (Figure 7B [↗](#)). The results were further consolidated by immunofluorescence as the nuclear localization of Chk1, Chk2, BRCA2, Rad51, and Artemis increased in MG132 treated H357-R *POLK* KO cells (Figure 7C [↗](#) and Supp. Fig. 7A [↗](#)). Thus, the absence of protein bands in Polk depleted cells are mostly likely due to proteasomal degradation and Polk could enhance the stability and cellular availability of these critical DDR proteins.

## Dysregulation of proteasomal degradation and deubiquitinating systems in cisplatin resistant OSCC

To delineate the possible molecular mechanism by which Polk is able to protect ubiquitin-mediated degradation of critical DDR proteins, we reanalyzed publicly available RNA-seq data of H357-S and H357-R cells [ArrayExpress (E-MTAB-9697)]. The total dysregulated genes were accessed, and STRING analyses was carried out. Interestingly, in addition to several altered pathways, around 349 genes are involved in the protein degradation pathway were dysregulated (Figure 8A i-iv [↗](#), Supp. Table-4 a and b [↗](#)). Out of which, 76 and 8 genes involved in ubiquitination pathways (e.g., *UBC*, *ISG15*, *RNF185*, and *ATG10*, etc.) and 20S proteasomal complex formation (*PSMB5*, *PSMB10*, *PSMC1*, *PSMC5*, *PSMD6*, *PSMD9*, *PSMD12*, and *PSME3*) were down-regulated significantly in H357-R than in H357-S cells. While 13 genes like *USP2*, *USP18*, *USP42*, *USP43*, and *OTUD3*, etc., involved in the removal of ubiquitin from their conjugates were up-regulated in H357-R cells. The rest of the genes were marginally dysregulated. Our RNA-seq analyses indicated that the protein degradation pathways are probably affected in the cisplatin resistant cells due to overall downregulation of the 20S proteasomal complex as well as upregulation of deubiquitinating enzymes. To validate it, semi-quantitative and real-time RT-PCRs for two deubiquitinase genes, *USP2* and *USP18*, and two proteasomal complex genes *PSMA7* and *PSMB5*, were carried out (Figure 8B [↗](#)). While *USP2* encodes a ubiquitin-specific protease of the C19 peptidase superfamily which deubiquitinates polyubiquitinated target proteins such as fatty acid synthase, MDM2, MDM4, and cyclin D1 (Davis et al. 2016 [↗](#)) (Tang et al. 2022 [↗](#); Zhu et al. 2022 [↗](#); Li et al. 2026 [↗](#)), *USP18* (alias *UBP43*) encodes a major ISG15-specific protease that efficiently and selectively cleaves ISG15 (a ubiquitin-like protein) fusions (D'Andrea and Pellman 1998 [↗](#); Geng et al. 2024 [↗](#)). *USP18* regulates several biological processes like immune cell development,

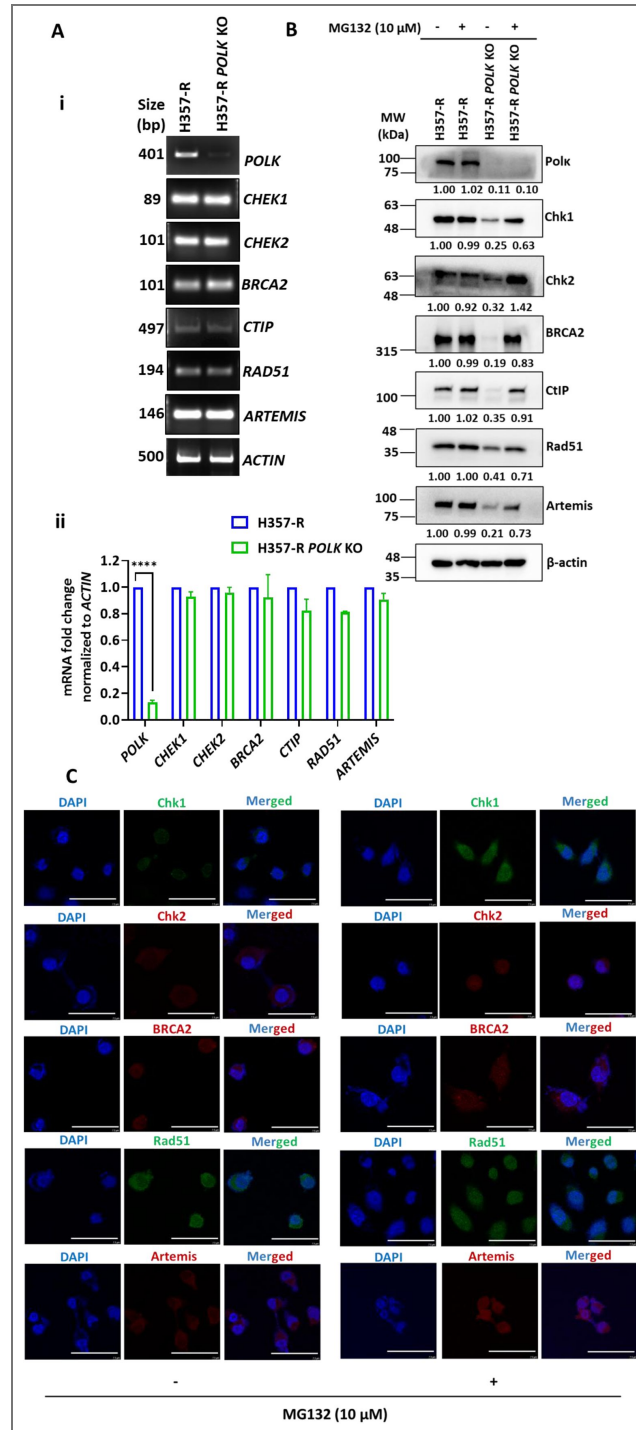


**Figure 7. Stabilization of proteins involved in checkpoint and DSB repair pathways from proteasomal degradation by Polk.**

(A) RT-PCR analysis of indicated genes was carried out in H357-R and H357-R *POLK* KO cells (i) and the mRNA expression levels were represented in bar graph (ii). Data were represented as mean ± SEM (n=2). Statistical significance determined by two-way ANOVA with Tukey's multiple comparisons test (\*\*\*\*p < 0.0001, and ns- nonsignificant). (B) Western blot analyses of cell lysates of H357-R *POLK* KO and H357-R *POLK* KO cells without and treated with 10 μM of MG132 for 6 hours was conducted and probed with indicated antibodies. β-actin was used as a loading control. Densitometric fold change relative to proteins in H357-R cells has been provided just below each band. (C) Representative immunofluorescence images of H357-R *POLK* KO and H357-R *POLK* KO cells treated with 10 μM of MG132 show DAPI (blue), Chk1 (green), Rad51 (green), Chk2 (red), BRCA2 (red), and Artemis (red), and corresponding merged images. Scale bars indicate 7.5 μm.

autoimmune diseases, pathogens response, and tumor development (Honke et al. 2016 [↗](#)). *PSMB5* (Proteasome Subunit Beta Type-5) encodes a catalytic subunit of the 20S proteasome core complex, crucial for protein degradation in eukaryotes (Oerlemans et al. 2008 [↗](#)). *PSMA7* (Proteasome Subunit Alpha Type-7) encodes a critical structural component of the 20S proteasome core complex, and as an alpha subunit, it forms the “gateway” of the proteasome, regulating the entry of proteins into the catalytic core for destruction (Wu et al. 2021 [↗](#)). We selected these four genes for further analysis as these are highly altered and reported to be involved in promoting several tumors development, their progression and chemoresistance. Total cDNA was synthesized from the RNA isolated from H357-S, H357-R, and H357-R *POLK* KO cells. Endpoint reverse transcription and qRT PCR results revealed ~2-4 fold higher expression of *USP2* and *USP18* in H357-R cells. *PSMB5* and *PSMA7* mRNA expression was somewhat less in H357-R cells but ~3-fold more in H357- *POLK* KO cells. To strengthen it further, expression of these proteins was checked using specific antibodies (Figure 8C [↗](#)). H357-R cells exhibited increased expression of *USP2* and *USP18* and reduced levels of *PSMA7* and *PSMB5* compared to other cells. These findings suggest that decreased ubiquitination, together with enhanced *USP2/USP18* deubiquitinase activity, may contribute to the stabilization of key cell cycle checkpoint and DNA damage response (DDR) proteins. This, in turn, likely facilitates replication fork protection and restart, thereby promoting cisplatin resistance in OSCC-R cells.

## PCNA-Polκ-USP18 axis plays an important role in DDR proteins stabilization and chemoresistance in OSCC

Next, we checked any physical and functional interaction between Polκ and deubiquitin enzymes that regulate stabilization of critical DDR proteins and cisplatin resistance in OSCC by immunoprecipitation and nuclear co-localization. The complete cellular extract was either precipitated by anti-Polκ or anti-PCNA, and the pulling down of *USP2* and *USP18* proteins was detected by respective antibodies. While immunoprecipitation with IgG beads did not precipitate any proteins, in both approaches, we could observe a positive interaction between Polκ, PCNA, and *USP18* (Figure 9A [↗](#) and Supp. Fig. 7B [↗](#)). Immunoprecipitation either with *USP2* or Polκ antibodies could not pull down the other partner, suggesting no interaction between the two. Moreover, we also could not detect the interaction of *USP2* with PCNA. The nuclear co-localization analysis also confirmed similar results (Figure 9B [↗](#)). To investigate how *USP18* depletion affects protein stability, *USP18* expression was silenced in H357-R cells using specific siRNA, followed by analysis of key DNA damage response (DDR) proteins by Western blotting. We observed that upon knocking down *USP18*, the protein stability of Chk1, Chk2, CtIP, and Artemis reduced significantly, similar to Polκ depletion, but recovered only when a proteasomal inhibitor was added to the cells (Figure 9C [↗](#)). This result suggested that loss of *POLK* or *USP18* in H357-R cells renders a similar fate of the DDR proteins, which is likely to affect replication fork protection and restart in the presence of cisplatin. MTT assays further showed that cisplatin sensitivity was enhanced upon *USP18* knock down (Figure 9D [↗](#)). Since Polκ seems to be the master regulator of several pathways to induce chemoresistance, by targeting this TLS Pol the efficacy of cisplatin can be improved. As Polκ's interaction with PCNA is indispensable for such a role, the binding site between the two proteins may be targeted. We leveraged an existing small molecule T2AA that binds to the interdomain connecting loop (IDCL), where usually most of the DNA Pols bind. Polκ binds to the IDCL of PCNA, since T2AA is a generic inhibitor and can prevent binding of all other Pols, it inhibited the cell survival of H357-S, H357-R, and H357-R *POLK* KO cells, *albeit* more in H357-S and H357-R *POLK* KO cells (Figure 9E [↗](#)). The addition of cisplatin further heightened the sensitivity of H357-S and H357-R *POLK* KO cells. A specific small molecule that can disrupt PCNA-Polκ interaction will be much more relevant for clinical use. Also an inhibitor of *USP18* may also improve the reversal of cisplatin resistance of OSCC cells and that require further investigation. Nevertheless, this study identified yet another tripartite axis of PCNA-Polκ-USP18 that is involved in stabilizing the genome of a highly proliferating cell under cisplatin stress and can be targeted for novel chemotherapeutics development.

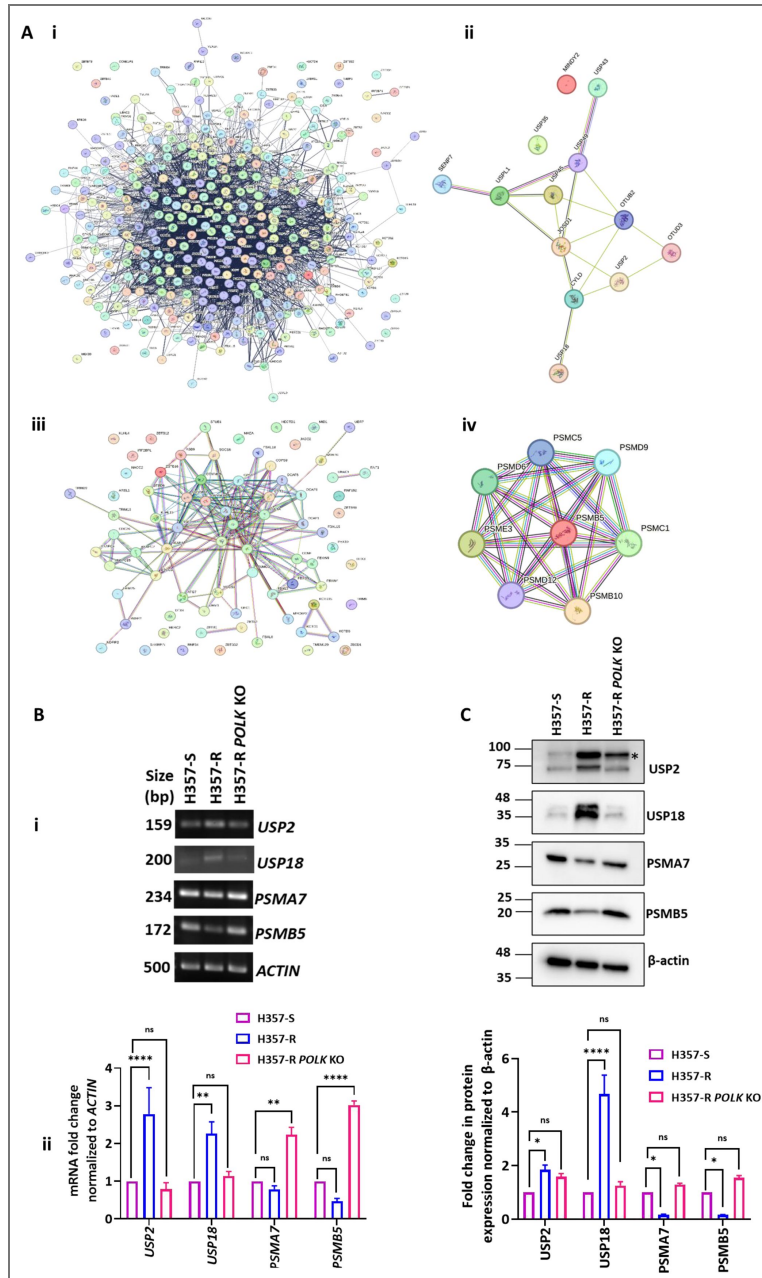


**Figure 8. Dysregulation of proteasomal degradation and deubiquitinating systems in cisplatin resistant OSCC.**

(A) A comparative transcriptomics data of H357-S and H357-R was retrieved and re-analyzed. String analysis revealed a total of 349 dysregulated genes of protein degradation pathways (i), out of which 13 genes are significantly up-regulated deubiquitination pathways (ii), 76 genes are down-regulated involved in ubiquitination pathways (iii), and 8 genes are down-regulated those are components of 26S proteasomal complex (iv). (B) Endpoint RT-PCR analysis of indicated genes was carried out in H357-S, H357-R and H357-R POLK KO cells (i) and qRT-PCR gene expression analysis of the indicated genes in H357-S, H357-R and H357-R POLK KO cells using SYBR Green. ACTIN was used as a control.  $\Delta\Delta ct$  values were calculated and compared for the H357-S, H357-R and H357-R POLK KO cells. Calculated fold change was plotted. Data were represented as mean  $\pm$  SEM (n=3) (ii). Statistical significance was determined by two-way ANOVA with Tukey's multiple comparisons test (\*\*p < 0.01, \*\*\*\*p < 0.0001, and ns- nonsignificant). (C) Western blot analyses of H357-S, H357-R and H357-R POLK KO lysate were carried out and probed with indicated antibodies.  $\beta$ -actin was used as a loading control. (\*) indicates a non-specific band for USP2 antibody. USP18 antibody detected two sizes of the protein. Fold change in protein expression was shown in a bar graph. Data represented as mean  $\pm$  SEM (n=2). Statistical significance was determined by two-way ANOVA with Tukey's multiple comparisons test (\*p < 0.05, \*\*\*\*p < 0.0001, and ns- nonsignificant).

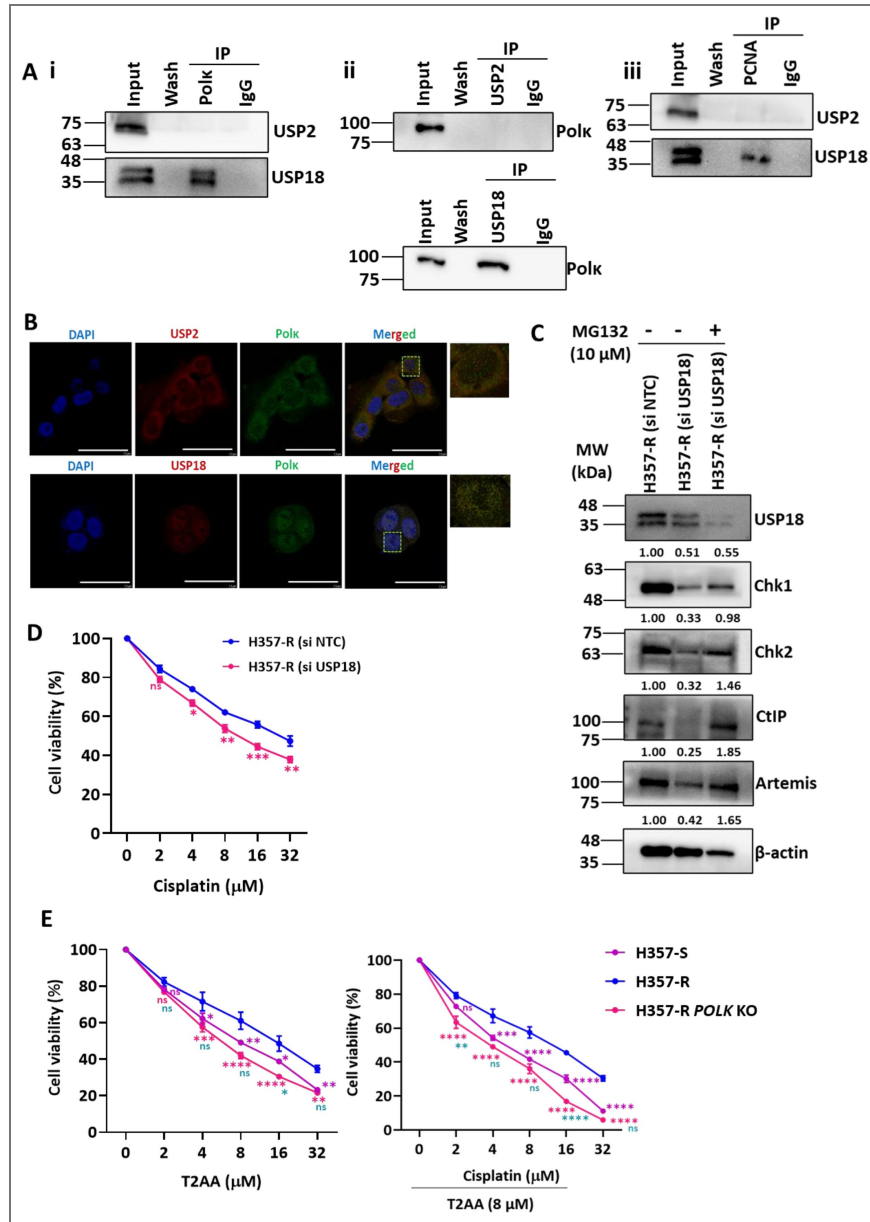


**Figure 9. PCNA-Polk-USP18 axis stabilizes DDR proteins.**

(A) Co-immunoprecipitation was performed in H357-R whole cell extract using either Polk (i) or USP2 and USP18 antibodies (ii). Similar interaction between PCNA with USP2 and USP18 was determined. IgG was considered as a negative control. Representative best immunoblots from two independent experiments are shown. (B) Immunofluorescence co-localization analysis of H357-R cells showed USP2 (red), USP18 (red), Polk (green), DAPI (blue), and corresponding merged images. Merged images represent co-localization of USP2 and USP18 with Polk in the nucleus. Zoom-in merged (only green and red) view of dashed box area showed in upper right corner of corresponding image. (C) Western blot analyses of cell lysates of H357-R, MG132 untreated and treated H357-R USP18 knockdown cells were carried out and expression levels of indicated proteins were determined. Densitometric fold change relative to β-actin has been provided just below each band. (D) Cells were treated with the indicated concentrations of cisplatin for 48 hours and then an MTT assay was performed. The graph indicates the mean ± SEM (n=3), and statistical significance was determined by two-way ANOVA, Šídák's multiple comparisons test, (\*p < 0.05, \*\*p < 0.01, \*\*\*p < 0.001, and ns-nonsignificant). Pink asterisks indicate comparison between H357-R (si NTC) to H357-R (si USP18). (E) H357-S, H357-R and H357-R POLK KO cells were treated with the indicated concentrations of T2AA alone and with cisplatin were treated for 48 hours and then an MTT assay was performed. Graph indicates the mean ± SEM (n=3), two-way ANOVA with Tukey's multiple comparisons test (\*p < 0.05, \*\*p < 0.01, \*\*\*p < 0.001, \*\*\*\*p < 0.0001, and ns-nonsignificant). Purple asterisks indicate comparison between H357-R to H357-S, pink asterisks indicate comparison between H357-R to H357-R POLK KO, and green asterisks indicate comparison between H357-S to H357-R POLK KO.

## Discussion

DNA replication immortality is one of the critical hallmarks of cancerous cells that helps in continuous proliferation, invasion, and insensitiveness to chemo- and radio-therapeutics (Swanton et al. 2024 [↗](#)). The efficacy of cisplatin is compromised because of evolving intrinsic and acquired resistance mechanisms (Dasari and Tchounwou 2014 [↗](#)). The resistance to cisplatin by various tumors has been reported to require TLS activities of Pol $\eta$ , Rev1, and Pol $\zeta$ , where the former Pol acts as an inserter and others as mismatch extenders to maintain continuous replication and cell proliferation (Sharma et al. 2012 [↗](#); Zhao et al. 2012 [↗](#); Yoon et al. 2021 [↗](#)). The role of the other two TLS Pols-  $\kappa$  and  $\iota$  in cisplatin resistance is poorly established. This study revealed that Pol $\kappa$  is overexpressed exclusively in head and neck cancerous cells upon cisplatin treatment and also in cisplatin resistant oral squamous cell carcinoma cells. Other reports also suggested upregulation of Pol $\kappa$  in lung, ovarian, glioma, and prostate cancers, and its downregulation in stomach, colorectal, and breast cancers in comparison to the normal neighboring tissues associated with tumorigenesis, disease progression, and resistance to various therapeutics (Pillaire et al. 2014 [↗](#); Peng et al. 2016 [↗](#)). According to the GCO (Global Cancer Observatory), the incidence of OSCC was standing at 377,713 cases in 2020, which is believed to be increased to 40% by 2040 (Tan et al. 2023 [↗](#)). OSCC treatments require surgery followed by, if necessary, radio- or chemo-therapy. The chemotherapeutics include cisplatin, alone or in combination with 5- fluorouracil and docetaxel (TPF). But due to THE development of chemoresistance, patients experience relapse, which leads to continued tumor growth and metastasis. Thus, understanding the mechanism of cisplatin resistance is key to the identification of adjunct targets and drug discovery for better OSCC management. We exploited available cisplatin resistant OSCC and explored and determined the underlying mechanisms of Pol $\kappa$ 's involvement in cisplatin resistance, and further suggested a few therapeutic targets (Figure 10 [↗](#)).

*TLS independent function of Pol $\kappa$  stabilizes the cell's genome to induce cisplatin resistance:* The reversal to re-sensitization of resistant HNSCC cells to cisplatin upon *POLK*'s absence suggested that Pol $\kappa$  could play an important role in the bypass of cisplatin adducts in these cells. As a consequence of *POLK* deletion, OSCC-R cells accumulated DNA breaks and increased  $\gamma$ H2A.X expression, followed by a slowing down of cell cycle progression that resulted in PARP-1 cleavage and enhanced cell death, suggesting the importance of Pol $\kappa$  in genome stability in the presence of cisplatin. The involvement of this polymerase in replication fork protection and recovery was again demonstrated in the DNA fiber assay. More accumulation of stalled and collapsed forks and slower moving ongoing forks in *POLK* knockout cells than the cisplatin resistant cells harboring abundant Pol $\kappa$  further strengthened the critical role of this TLS polymerase in lowering cisplatin toxicity. Interestingly, for such a function of Pol $\kappa$ , the catalytic activity was dispensable, but its PCNA interaction motifs were required. Thus, we concluded that the non-TLS activity Pol $\kappa$  induces cisplatin resistance in OSCC. Yet another study reported that Pol $\kappa$  gets overexpressed in melanoma, lung, and breast cancer cells, which helps in cellular proliferation in response to oncogenic alterations, specific kinase inhibition, oxidative stress, or starvation. Additionally, it enhances the resistance of A375 melanoma cells to the BRAF-targeted inhibitor vemurafenib; thus, targeting Pol $\kappa$  may reduce drug resistance in such cancer patients. The study even proposed a noncatalytic function of Pol $\kappa$  to explain the drug resistance (Temprine et al. 2020 [↗](#)). Another report has also demonstrated a noncatalytic function of Pol $\kappa$  in DNA damage response (Kanemaru et al. 2015 [↗](#)). Ectopically overexpressed catalytically dead Pol $\kappa$  mutant in human lymphoblastic Nalm6 cells rendered similar sensitivity to hydrogen peroxide and menadione as the wild-type cells, whereas the respective Pol $\kappa$  knockout cells exhibited severe sensitivity, although the underlying mechanisms by which the catalytically deficient Pol $\kappa$  protected against such damage remained unexplored. However, another study suggested that Pol $\kappa$  induces ATR-CHK1 activation (Peng et al. 2016 [↗](#)). Thus, Pol $\kappa$ 's non-catalytic activities are critical to multiple cancer drug resistance in several tumor types.

*Pol $\kappa$  maintains cellular homeostasis of critical checkpoint and DNA break repair proteins:* Next, we presented several compelling evidence supporting non-catalytic roles of Pol $\kappa$  in cellular homeostasis by regulating the abundance of critical proteins involved in checkpoint activation

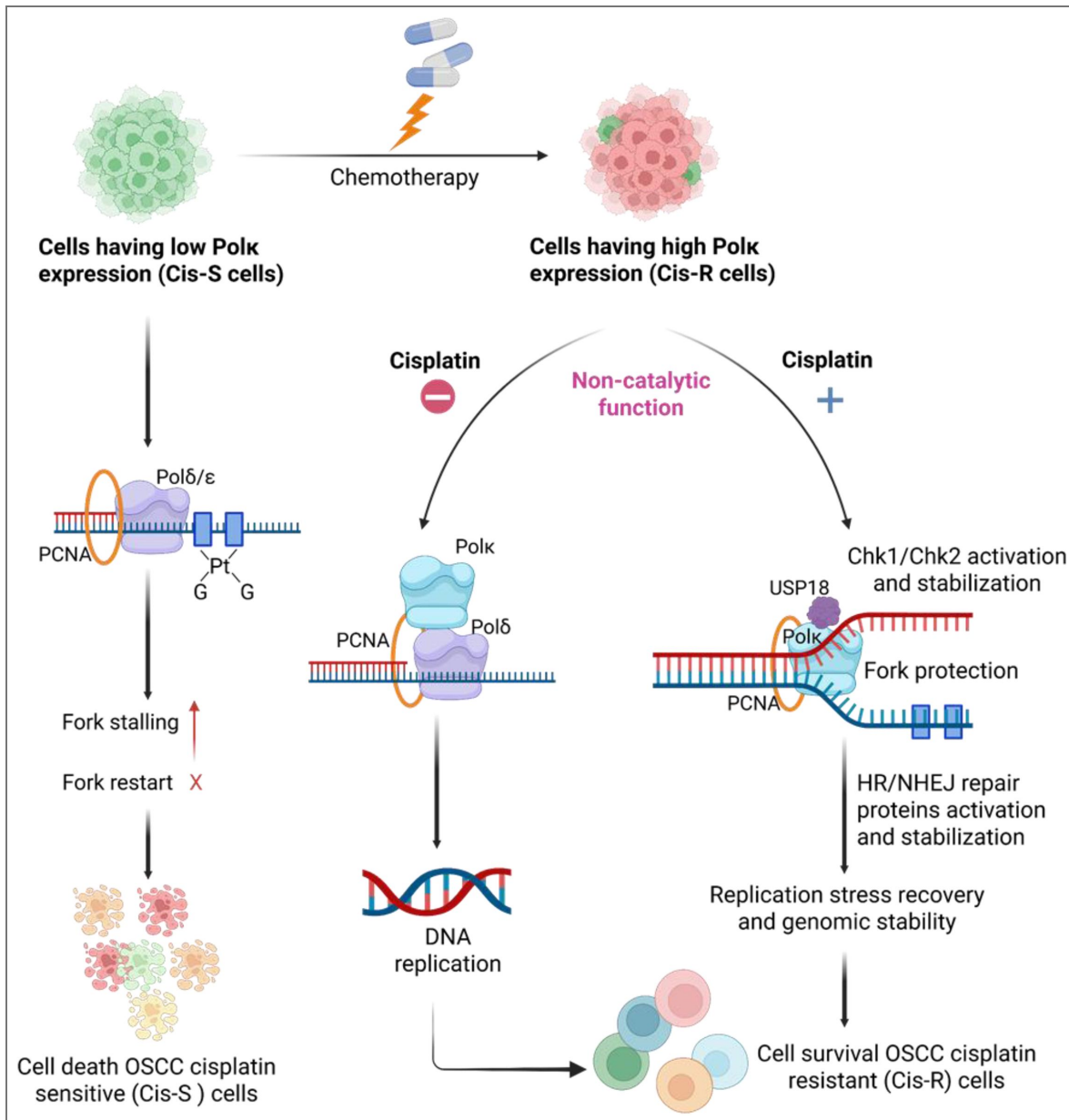


**Figure 10. Dual tripartite interactions mediated by Polk govern uninterrupted DNA replication and genome stability in OSCC cisplatin resistant cells.**

In the cells having low Polk expression the bulky adducts generated by cisplatin could not be bypassed leading to more fork stalling and collapse, which ultimately leads to cell death. Whereas in cisplatin resistant cells where Polk is overexpressed, it modulates two axes independent of its catalytic activity. The PCNA-Polk-Polδ axis facilitates efficient replication and proliferation of cells, the other axis PCNA- Polk-USP18 stabilizes DNA damage response proteins to activate checkpoint and HR/NHEJ repair pathways during cisplatin exposure.

d DNA break repair pathways in human cells. For the first time, we showed that the depletion of Polk in OSCC-R cells (both H357-R and SCC9-R) induces a decrease in the protein levels of Chk1, Chk2, p-Chk1, and p-Chk2 of ATM-ATR; CtIP, BRCA1, BRCA2, Rad51, and RAD54 of HR; and DNA-PKCs, Artemis, and DNA ligase IV of NHEJ pathways. Although we have not checked other proteins of these pathways, it appears that only the downstream proteins are affected upon Polk depletion. In the presence of a proteasome inhibitor, the protein levels of these get recovered in *POLK-KO* cells, again suggesting the role of Polk in regulating proteasomal degradation of these critical proteins. Contrarily, in OSCC-R cells, Polk overexpression maintains critical cellular abundance of these proteins to protect the replication fork and further repair by these pathways to overcome cisplatin toxicity. DNA replication stress is nothing but the slowing or stalling of replication fork progression, resulting in DNA synthesis inhibition. The cellular response to replication stress requires activation of the ATR/Chk1 and ATM/Chk2 checkpoint axes, which sense the slow moving and stalled replication forks (Kumari et al. 2025 [\[3\]](#)). Their activation allows protection of the fork from nucleases like MUS81 and MRE11, and repair by selective repair pathways, prevents firing of late replication origins, and inhibits further progress to mitosis until the completion of replication (Gonzalez Besteiro and Gottifredi 2015 [\[3\]](#)). Under normal physiological conditions, the ablation of Chk1 inhibits the replication rate. Accordingly, *CHEK1* knockout mice do not survive, and its haploinsufficiency enhances genome instability and mutagenesis (Stancel et al. 2009 [\[3\]](#)). During the course of this study, yet another report suggested stabilization of only Chk1 specifically by Polk, independent of its polymerase activity, in four different cell lines, such as MRC5-SV, 293T, HCT116, and RKO (Dall'Osto et al. 2021 [\[3\]](#)). In that report, the expression levels of Chk2, and proteins of HR, and NHEJ pathways were not explored. The replication fork restart defects associated with Polk depletion can be rescued by Chk1 overexpression (Forment et al. 2011 [\[3\]](#); Thompson et al. 2012 [\[3\]](#)). However, how Polk protects Chk1 from proteasomal degradation was not determined until this study. The *CHEK1* expression at the transcriptional level is known to be p53 dependent (Gottifredi et al. 2001 [\[3\]](#)). Since the mRNA level of *CHEK1* remained unaltered in the Polk knockout cells whereas its protein expression was affected, it suggested that the regulation of Chk1 expression is p53 independent but Polk dependent. Chk2 is a central transducer of the DNA damage response (DDR) that gets activated by ATM upon DNA damage to stop cell cycle progression (at G1/S or G2/M phases) and induces DNA repair or apoptosis (via p53). Chk2 also takes part in various cellular functions without the presence of any nuclear DNA lesions (Zannini et al. 2014 [\[3\]](#)). Upon its activation, Chk2 phosphorylates nearly 24 nuclear proteins including BRCA1, BRCA2, etc., involved in DDR (Seo et al. 2003 [\[3\]](#)). BRCA1 phosphorylation by Chk2 recruits Rad51 to the lesion sites and that promotes DNA strand invasion and the exchange steps of HR (Ciccia and Elledge 2010 [\[3\]](#)). Whereas BRCA2 phosphorylation causes disruption of Rad51-BRCA2 complex, also allowing Rad51 to bind lesion sites (Bahassi et al. 2008 [\[3\]](#); Saxena et al. 2019 [\[3\]](#)). No syndromes or cancer predisposition in mice have been linked to the Chk2 absence, although *CHEK2*<sup>-/-</sup> mice are more susceptible to skin tumors (Hirao et al. 2002 [\[3\]](#)). NHEJ is the primary, relatively low-fidelity repair mechanism for double-strand breaks in mammals, active throughout the cell cycle but crucial in G1, and involves proteins like Ku70/Ku80, DNA-PKCs, DNA Ligase IV/XRCC4, etc. While NHEJ directly repairs DNA double-strand breaks without a template, Chk2 manages cell cycle arrest to allow sufficient time for this repair. Since some of these proteins in ATR-Chk1, ATM-Chk2, HR, and NHEJ axes are stabilized in OSCC-R cells in a Polk-dependent manner, we propose that while ATR-Chk1 is critical for replication stress management by preventing fork degradation and break accumulation without cisplatin, the ATM-Chk2, axis along with HR and NHEJ pathways may efficiently repair cisplatin adducts.

*A Polk-Polδ-PCNA tripartite axis promotes efficient DNA replication of OSCC-R cells:* Apart from TLS, the involvement of DNA polymerase kappa has also been implicated in the progression of replication forks through intrinsic natural barriers where replicative Pols find difficulty in synthesizing DNA (Barnes et al. 2017 [\[3\]](#)). Common fragile sites (CFSs) are usually enriched in repetitive DNA sequences and are difficult to replicate; therefore, they are unstable genomic loci that altered frequently in cancers. Biochemical assays revealed that Polk replicate CFS-mimicking sequences more efficiently than Polδ. A recent study using Polk sequencing revealed that Polk activity is required for the replication of euchromatin regions, GC-rich regions, promoters, and in

DNA that is replicated early in the S phase of DNA replication (Tang et al. 2024 [↗](#); Torres et al. 2024 [↗](#)). Polk is also required to protect and to restart the replication forks following starvation of deoxynucleoside triphosphates (dNTPs), regulated by both the Fanconi Anemia (FA) pathway and PCNA polyubiquitination (Tonzi et al. 2018 [↗](#)). All these reports suggested that Polk's role is not limited to only damage sites and plays multiple cellular functions as well. The colony counting, Comet and fiber assays, cell cycle analysis, and cell survival of OSCC-R cells in the presence of replication inhibitors like HU, Aphidicolin, and Camptothecin in this study further strengthen the role of Polk in regulating replication stress tolerance and fork progression. However, contrary to the *in vitro* DNA replication assay using CFS template, we observed that in this context as well, the catalytic activity of Polk is not required. A cooperative tripartite interaction between Polk-PCNA-Pol $\delta$  seems to be critical for the high proliferative ability of OSCC-R cells. In fact, studies showed that the depletion of Polk is associated with increased rates of spontaneous mutagenesis and inflammation in mice (Stancel et al. 2009 [↗](#); Hakura et al. 2019 [↗](#)). Thus, Polk plays a critical role in minimizing replication stress by stabilizing Pol $\delta$  or possibly other replicative DNA Pols on the replication fork and by activating the ATR-Chk1 pathway to protect stalled replication forks at the difficult replication sites.

*Polk-USP18 axis promotes efficient replication of cisplatin adducts in the genome of OSCC-R cells:* So far, we have established the role of Polk in genomic DNA replication without genotoxic stress and protection of replication fork by activation of ATR-Chk1, ATM-Chk2, HR, and NHEJ pathways by regulating their protein stability to cause cisplatin resistance. Ubiquitylation and deubiquitylation play important roles in regulating DNA repair pathways by coordinating the recruitment and removal of repair proteins at and from the damaged site (Messick and Greenberg 2009 [↗](#); Borsos et al. 2020 [↗](#); Sharma et al. 2020 [↗](#); Tang et al. 2021 [↗](#)). Reports suggested that Chk1 function is regulated by ubiquitination by the cullin-ring E3-ubiquitin ligases CUL1, CUL4A, and HUWE1 conjugating systems and deubiquitination by ubiquitin hydrolases like USP1, USP3, USP7, and ataxin3, which deubiquitinate Chk1 (Zhang et al. 2005 [↗](#); Zhang et al. 2009 [↗](#); Guervilly et al. 2011 [↗](#); Alonso-de Vega et al. 2014 [↗](#); Tu et al. 2017 [↗](#); Cheng and Shieh 2018 [↗](#); Cassidy et al. 2020 [↗](#)). Similarly, Chk2 ubiquitination is controlled by Cullin 1, PIRH2, and SIAH2, and deubiquitination by USP7 and USP39 (Lovly et al. 2008 [↗](#); Bohgaki et al. 2013 [↗](#); Garcia-Limones et al. 2016 [↗](#); Wu et al. 2019 [↗](#); Liu et al. 2024 [↗](#)). E3 ligases like RNF8, RNF168, and BRCA1 is a crucial post-translational modification regulating DNA double-strand break (DSB) repair by recruiting repair factors, such as 53BP1 and BRCA1, to damage sites. Specific E3 ligases like RFWD3 and RNF4 are responsible for ubiquitin-mediated degradation of RPA and Rad51 proteins to manage their turnover during homologous recombination. At least 15 of USPs (USP1, USP10, USP11, USP15, USP20, USP26, USP29, USP3, USP37, USP4, USP42, USP44, USP6, USP7, and USP51) have been demonstrated to regulate DSBR. These USPs can promote or suppress the choice of a DSBR pathway. Our transcriptional analysis of RNA-seq data of OSCC-R revealed upregulation of certain DUBs and downregulation of proteins involved in ubiquitin-mediated proteasomal degradation. We proposed that by preventing the degradation of key proteins involved in DDR, OSCC-R cells could efficiently nullify the cisplatin effect. Although we could not explore a direct role of Polk in the downregulation of 26S proteasomal proteins, we could show a direct association of Polk with USP18 deubiquitinase possibly via its UBZ domain in regulating a critical mass of proteins that get affected in the absence of Polk. For the first time, we reported a PCNA-Polk-USP18 deubiquitinating system in replication fork protection and restart, which is responsible for chemoresistance. A recent study already demonstrated the role of USP2 that deubiquitinates NBS1 and increases the stability of the MRN complex (MRE11-RAD50-NBS1) during the DSB response (Kim et al. 2023 [↗](#)). However, USP2 may function independently of Polk, as we did not see any physical interaction between the two proteins. There are several studies highlighted the importance of ubiquitination/deubiquitination systems in governing tumor behaviors in terms of tumor proliferation, migration, invasion, and resistance to therapeutic (Sharma and Almasan 2020 [↗](#); Chen et al. 2022 [↗](#); Zhang et al. 2023 [↗](#)). In similar lines, this study also found reversal of chemoresistant phenotype in OSCC-R cells by depleting USP18.

*Implication of Polk as a chemotherapeutic target:* Due to the central roles of TLS Pols in mutagenesis and cell survival post DNA damages, they have emerged as potential targets for the development of anticancer drugs that can be used as a solo or in combination with the existing therapy. For example, small molecule inhibitors against human Rev1 have been designed that target its interacting surface with Pol $\zeta$  and other TLS Pols, and some are being considered for clinical trials (Dash et al. 2018 [↗](#); Wojtaszek et al. 2019 [↗](#); Chatterjee et al. 2020 [↗](#); Yoon et al. 2021 [↗](#)). However, targeting Rev1 for cancer treatment may not be a viable option as it will inhibit TLS of all types of lesions in normal cells, and the inhibitor will increase cytotoxicity and tumorigenicity. Although Pol $\eta$  and Pol $\zeta$  are involved in cisplatin resistance, suitable inhibitors against these polymerases are yet to be identified and validated as chemotherapeutics (Korzhev and Hadden 2016 [↗](#); Patel et al. 2021 [↗](#)). This study unveils multiple non-conventional roles of Polk in replication fork stabilization, efficient replication restart, checkpoint activation, and cellular homeostasis of critical proteins of DSBR to induce cisplatin resistance by using various axes. Since the catalytic activity of Polk is dispensable for most of these phenotypes, a specific small molecule that can block its interaction with PCNA, rather than an existing generic inhibitor T2AA, can be designed and explored as adjunct therapy. Additionally, effective USP18 inhibitors can also be explored as additional therapeutics.

## Materials and Methods

### Cell lines and cell culture

Various human transformed cell lines such as A549 (non-small cell lung cancer), HEK293 (embryonic kidney), MCF7 and MDA-MB-231 (breast cancer), MIA PaCa-2 (pancreatic cancer), SH-SY5Y (Neuroblastoma), DU145 (prostate cancer), H357 and SCC9 (tongue OSCC) and Huh-7 (hepatoma) are maintained and grown appropriately, and used regularly in our laboratory (Khandagale et al. 2019 [↗](#); Sahu et al. 2024 [↗](#); Sahu et al. 2026 [↗](#)). The cisplatin resistant OSCC counter parts were developed in Dr. Rupesh Dash's laboratory (Maji et al. 2019 [↗](#)). Briefly, A549, HEK293, MCF7 and MDA-MB-231, SH-SY5Y, Huh-7, MIA PaCa-2 and DU145 cells were cultured in Dulbecco's Modified Eagle Medium (DMEM) from Hi-Media (Cat#AL007A). H357, SCC9 cell lines were cultured in Dulbecco's Modified Eagle Medium / Nutrient Mixture F-12 Ham [DMEM / F12, 1:1] from Hi-media (Cat#AL139A). All culture media were supplemented with 10% FBS (Gibco, Cat# A5256701), 1% penicillin-streptomycin (PS from Gibco, Cat#15140122), except for SH-SY5Y, where 15% FBS was added. For Huh7 and SH-SY5Y culturing, additionally MEM non-essential amino acids (Gibco, Cat# 11140-050) were supplemented. Similarly, 0.5 $\mu$ g/ml sodium hydrocortisone (Sigma, Cat# H6909) was added to the medium of the H357/SCC9 culture. All cell lines were kept in a 37°C incubator with 5% CO<sub>2</sub> and 95% relative humidity.

### Drug supplements, oligonucleotides and antibodies

cis-Diammineplatinum(II) dichloride (Cat#P4394), T2AA (Cat#SML0794), PCNAI1 (Cat# SML0730) and Camptothecin (Cat#C9911) were purchased from Sigma-Aldrich. MG132 (Cat#A2585) was sourced from ApexBio. Aphidicolin (Cat#38966-21-1) and Hydroxy urea (Cat#H0310) were procured from MP Biomedicals and TCI, respectively. List of primers used in this study were provided in [table 1](#) [↗](#) and antibodies in [table 2](#) [↗](#).

### Generation of *POLK* knockout cell lines

*POLK* gene knockout in H357-R cells was achieved using CRISPR/Cas9 gene targeting approach as recommended by Santa Cruz Biotechnology. Cells were co-transfected with the human *POLK* CRISPR/Cas9 KO plasmid (Cat#sc-405052) and its HDR plasmid (Cat# sc-405052-HDR) using Viafect transfection reagent (Promega, Cat#3498). The CRISPR plasmid pool contained three individual guide RNAs along with a Cas9 nuclease expression gene, while the HDR plasmid facilitated homologous recombination repair at the targeted loci, introducing a Red Fluorescent Protein (RFP) gene and a puromycin resistance gene. Transfectants were subjected to selection in a medium containing 2 $\mu$ g/ml puromycin for 48 hours.

**Table 1.** List of oligonucleotides used in the study.

Primers	Sequence (5'-3')
<i>POLQ</i> (FP)	TA CAA GTG AAG GGA GAT GAG G
<i>POLQ</i> (RP)	TCA GAG GGT TTC ACC AAT CC
<i>POLD1</i> (FP)	GGT GCT CAC GGG CAA GGC GGG CGG CGC TGC AGC CTT CGC CAA ACG
<i>POLD1</i> (RP)	ATC CTC ACC AGG CCT CAG GTC CAG GGG GTC C
<i>POLB</i> (FP)	TGC AGA GTC CAG TGG TGA CAT G
<i>POLB</i> (RP)	ATG AAC CTT TTG TAA CTG CTC CAC
<i>POLL</i> (FP)	CCA CTG CCC CTC GAA GAA T
<i>POLL</i> (RP)	TCC CAG CAC CAC CAG CTG C
<i>POLM</i> (FP)	TTC CCC ACT TTG GAG AAC AC
<i>POLM</i> (RP)	GTA CCA CCG GTC AGC AGT CT
<i>POLH</i> (FP)	GCG GTG ACA GCC ACT AAG
<i>POLH</i> (RP)	GTA ATG AGG GCT TGG ATG G
<i>POLI</i> (FP)	CA CTA AAT ACT GCT AAG AAA GGG C
<i>POLI</i> (RP)	TCC ACT TGG TAG GAA ATC CCG
<i>POLK</i> (FP)	AGA CTT AAG GGT AGA ACT GTT ACC
<i>POLK</i> (RP)	AAT GTA TCT TGG TGA CTC CA
<i>REV1</i> (FP)	TTG TGA TGA AGC GCT GGT AG
<i>REV1</i> (RP)	TTG GTC ACT AGC TGG CCT CT
<i>REV7</i> (FP)	CGA GTT CCT GGA GGT GGC TGT GCA TC
<i>REV7</i> (RP)	CTT GAC GCA GTG CAG CGT GTC CTG G
<i>CHEK1</i> (FP)	GGT GCC TAT GGA GAA GTT CAA
<i>CHEK1</i> (RP)	TCT ACG GCA CGC TTC ATA TC
<i>CHEK2</i> (FP)	CGG ATG TTG AGG CTC AGC A
<i>CHEK2</i> (RP)	TAT GCC CTG GGA CTG TGA GG
<i>BRCA2</i> (FP)	GAA AAT CAA GAA AAA TCC TTA AAG GCT
<i>BRCA2</i> (RP)	GTA ATC GGC TCT AAA GAA ACA TGA TG
<i>CTIP</i> (FP)	TGT GGA AGC CCT AAC TCT GC
<i>CTIP</i> (RP)	ACG CCA GAA AAT GAG AAG GC
<i>RAD51</i> (FP)	GAG GTG AGC TTT CAG CCA GGC AGA
<i>RAD51</i> (RP)	TCT GGT TGT TGA TGC ATG GGC GA
<i>ARTEMIS</i> (FP)	ACA GGA GAC TTC AGA TTG GCG
<i>ARTEMIS</i> (RP)	CAC TCC TCC CGA CTT GGA ATT
<i>USP2</i> (FP)	ATG TCC CAG CTC TCC TCC A
<i>USP2</i> (RP)	CGG CTT GAA ACC AAG TTT CTC C
<i>USP18</i> (FP)	CCT GAG GCA AAT CTG TCA GT
<i>USP18</i> (RP)	CGA ACA CCT GAA TCA AGG AG
<i>PSMA7</i> (FP)	ATG ACA ACG TCT GCA TGG C
<i>PSMA7</i> (RP)	GCC TAG GAG TGC CAT CAA AGT
<i>PSMB5</i> (FP)	TCA TGG ATC GGG GCT ATT CC
<i>PSMB5</i> (RP)	AGA TCA GCC ACA TTG TCA CTG
<i>ACTIN</i> (FP)	TGT GAT GGT GGG AAT GGG TCA G
<i>ACTIN</i> (RP)	TTT GAT GTC ACG CAC GAT TTC C
<b>siRNA</b>	<b>Sequence (5'-3')</b>
siNTC	AUC ACC GAA CCG CUA ACC A
siPOLK	GCU CAA AUC ACC AGC CAAC
siUSP18	GGA AGA AGA CAG CAA CAU G

Antibodies	Source	Identifier
Polκ	Santa Cruz	SC-166667
Polη	CST	13848S
Polθ	Self-raised	n.a.
P125	Sigma	SAB4200053
Polβ	Santa Cruz	SC-376581
Polλ	Santa Cruz	SC-373844
Polμ	Santa Cruz	SC-398666
Polι	Santa Cruz	SC-101026
Rev1	Santa Cruz	SC-393022
Rev7	Santa Cruz	SC-47747
β-actin	Santa Cruz	SC-47778
γH2AX (S139)	CST	9718S
PARP1	CST	9542S
GFP	CST	2956S
ATR	CST	2790S
ATM	CST	2873S
P-ATR (Ser428)	CST	2853S
P-ATM (Ser1981)	CST	5883S
Chk-1	CST	2360S
Chk-2	CST	2662S
p-Chk1 (S341)	CST	2348S
p-Chk2 (T68)	CST	2661S
Mre11	CST	4895S
Rad50	CST	3427S
NBS1	CST	3002S
P-NBS1	CST	3001S
CtIP	CST	9201S
BRCA1	CST	14823T
BRCA2	CST	10741T
RAD54	CST	15016T

**Table 2.** List of antibodies used in the study

Rad51	CST	8875T
KU70	CST	4588T
KU80	CST	2180T
DNA PKCs	CST	38168T
P-DNA PKCs	CST	68716T
Artemis	CST	13381T
DNA LIG IV	CST	14649T
XLF	CST	2854T
XRCC4	CST	23908S
Histone H3	CST	14269S
Cleaved PARP1 (Asp214)	CST	9541S
p50	Sigma	SAB4200054
p12	Self-raised	n.a.
Ki 67	CST	12202
USP2	Proteintech	10392-1-AP
USP18	CST	4813S
PSMA7	Proteintech	15219-1-AP
PSMB5	CST	12919S

n.a.: Not applicable

**Table 2.** (continued)

A single cell was selected using fluorescence-activated cell sorting (FACS), placed in 96-well plates, and cultivated for 7-10 days to facilitate the development of individual colonies. Selected knockout clones were confirmed by Western blotting to verify successful *POLK* gene knockout.

## siRNA transfection and gene knockdown

Cells were seeded for 24 hours before transfection with 25nM siRNA (Eurofins) using Lipofectamine 2000 (Invitrogen). The following siRNA molecules were used; siNTC: 5'-AUC ACC GAA CCG CUA ACC A-3', si*POLK*: 5'-GCU CAA AUC ACC AGC CAAC-3', si*USP18*: 5'-GGA AGA AGA CAG CAA CAU G-3'. After 48 hours of transfection, cells were yielded for further experiments.

## Generation of plasmid constructs and over-expression

Amino terminal GFP tag constructs of wild type Polk and its PIP (F532A, L533A, F868A, F869A) and catalytically deficient (D198A, E199A) mutants were generated and designated as GFP-WT, GFP-PIP and GFP-CD, respectively. To generate the PIP mutant, the C-terminal portion harboring both mutated PIP motifs was amplified using 5'-CC CGG ATA TCT AGT TTT CCC AAT GAA GAG GAC AGG AAA CAC CAA CAA AGG AGC ATT ATT GGC GCT GCA CAG GCT GG-3' and 5'-GGCC AAG CTT GGA TCC TTA CTT GCA GCA TAT ATC AAG GG-3' primer pairs, digested with EcoRV and HindIII restriction enzymes and ligated into the same sites to replace the wild type fragment in pCMV-human Polk. Similarly, a ~2 kb fragment of having catalytically dead mutation was amplified using primers pairs 5'-TTT TAT GGC CAT GAG TCT TGC CGC GGC CTA CTT G-3' and 5'-AGC GGA TAA CAA TTT CA-3', digested with MscI and HindIII, and cloned into the same sites to replace the wild type fragment in pUC19-human Polk. BamHI fragments of these constructs were subcloned into the same site of PcDNA-GFP. Various construct of WT and mutants of Polk were transfected to H357-R *POLK* KO cells using FuGENE HD transfection reagent (Promega, Cat#E2311) according to manufacturer's instructions. After 48 hours of transfection, the cells were harvested for further experiments.

## RNA extraction and RT-PCR

Total RNA was purified using TRIzol (Ambion Life Technology, Cat#15596018). After purification, quality and concentration of RNA were checked using Nanodrop 2000, and cDNA was generated using an Applied Biosystems cDNA synthesis kit (Cat#4368814). Required gene of interests were amplified by RT-PCR; conditions included denaturation at 95°C, followed by 55°C for annealing and 72°C for extension. Bands were visualized by agarose gel electrophoresis, photographs were captured using BIO-RAD ChemiDoc MP imaging system, and examined using ImageJ software. For real time quantitative PCR, all reactions were performed in technical duplicates and biological triplicates by amplifying the gene of interest and *ACTIN* as an endogenous control with SYBR Green Master mix (Applied Biosystems, Cat#A25742) and QuantStudio 3 (Applied Biosystems). The  $\Delta\Delta Ct$  values were calculated and compared. Graphs were plotted using GraphPad Prism 9.0.0 software after calculating the fold change.

## Western blot analysis

Cells with 70-80% confluency were collected via trypsinization and then lysed on ice for 30 minutes with RIPA lysis buffer (CST, Cat#9806), a protease inhibitor cocktail (BioPioneer, Cat#BPBOI001), and phosphatase inhibitor cocktail (CST, Cat#5870S) with quick vortexing after every 5 minutes. Samples were centrifuged at 14,000 g for 20 minutes at 4°C, and supernatants were collected. Total protein concentration was measured using the Bradford assay. For nuclear extracts, protocol provided by Thermo Fisher Scientific with slight modifications was used. Briefly, cells ( $2 \times 10^6$ ) were collected and washed twice with ice cold 1X PBS. Cell pellet was resuspended in 200  $\mu$ l hypotonic solution (20 mM Tris-HCl (pH 7.4), 10 mM NaCl, 3 mM MgCl<sub>2</sub>) by pipetting up and down multiples times. Samples were kept on ice for 15 minutes, followed by 10  $\mu$ l of 10% NP-40 addition and vortexing for 10 secs at high speed, and then samples were centrifuged for 10 minutes at 5,000 rpm at 4°C. Supernatants were collected and saved as cytoplasmic fraction. The purity of cytoplasmic fraction was confirmed by checking the expression of GAPDH, as it is present in abundant in cytoplasmic fraction and absent or, minimal in nuclear fraction. Pellet was then

resuspended in 40  $\mu$ l of complete cell extraction buffer with high salt concentrations (400 mM NaCl). After 30 minutes on ice with vortexing in every 5 minutes, samples were centrifuged at 14,000 g for 20 minutes at 4°C. Supernatants were collected and saved as nuclear fractions and after protein estimation using Bradford's assay, about 40  $\mu$ g of total protein from each sample was boiled in SDS buffer at 95°C for 10 minutes and resolved on 7-12% of SDS-PAGE, and transferred to polyvinylidene difluoride (PVDF) membranes (Cytiva, Cat#10600023). To prevent non-specific binding, membranes were blocked with 5% non-fat dry milk (NFD, Hi-Media, Cat #GRM1254) or BSA (MP Biomedicals, Cat#160069) in TBS-T buffer [Tris-Buffered Saline with 0.1% Tween20 (Gene Tex, Cat#GTX03634)] at room temperature for 1.5 hours. Blots were then incubated with specific primary antibodies against various proteins at 4°C overnight on a rocking platform. After three washes with TBS-T, membranes were incubated for 1.5 hours at room temperature with HRP-conjugated secondary antibodies (1:5000) (anti-rabbit, Cat#A0545, anti-mouse Cat#A9044 and anti-rat Cat#A9037) from Sigma. Protein bands were visualized using a chemiluminescent HRP substrate ECL reagent (TaKaRa, Cat#T7101A) on a Chemi-Doc MP imaging system (BIO-RAD). Quantification of protein expression was done using Image J software.

## Immunoprecipitation

Various cells in 100-mm tissue culture dishes were grown. After 24 hours cells were collected by trypsinization and lysed in 400  $\mu$ l of 1X immunoprecipitation (IP) lysis buffer of Protein G immunoprecipitation kit (Sigma, Cat #IP50) containing Protease/Phosphatase Inhibitor Cocktail on ice. The lysate was centrifuged at 14,000 g for 20 minutes at 4°C. Supernatant protein concentration was determined using Bradford reagent (Sigma, Cat#B6916). Freshly prepared samples containing 500  $\mu$ g-1 mg of total protein were pre-cleared via incubation with protein G agarose beads (Sigma, Cat#IP50) for 4 hours at 4°C on a rotator and used for IP by incubating with anti-Pol $\kappa$  antibody, anti-PCNA, anti-USP2, anti-USP18, anti-Pol $\theta$  or, IgG control and 1X IP buffer to make up final volume to 600  $\mu$ l overnight at 4°C on a rotator. Immune complexes were then precipitated by protein G agarose beads at 4°C for overnight. Next day, the immunoprecipitates were washed 6 times with 700  $\mu$ l 1X IP lysis buffer on ice. Last wash was done with 0.1X IP buffer. Empty spin was given for 30 secs to remove any remaining buffer. Then samples were re-suspended in 40  $\mu$ l of 1X Laemmli sample buffer. The samples were separated by 10% SDS-PAGE and Western blot analysis was performed as described. Immunodetection was done using primary p50, p12, PCNA, Pol $\kappa$ , USP2 and USP18 antibodies and respective HRP-conjugated secondary antibodies (anti-mouse Cat#A9044, anti-rabbit Cat#A0545, anti-rat Cat#A9037) from Sigma. ECL reagent (TaKaRa, Cat#T7101A) was used for image development on Chemi-Doc MP system (BIO-RAD). Whole cell lysate (input) was also subjected to immunoblotting to detect the same protein expression as described.

## Colony forming assay

In the clonogenic survival studies, approximately 500 cells were seeded in each well of a 6-well plate or 35mm Petri-plates. After 24 hours, cisplatin was administered at indicated concentrations for 48 hours. After 48 hours, the media was replaced with complete growth media. Then cells were allowed to grow for a further 11–14 days; media change was done in every 2 days interval. The surviving colonies were fixed using 4% formaldehyde, treated with crystal violet stain (0.5%), and then images were captured using the BIO-RAD Chemi-Doc system and examined using ImageJ software.

## Annexin-V/PI assay

Cells were cultured in 6-well plates for 24 hours and subsequently treated with cisplatin (5  $\mu$ M). The Annexin V/PI flow cytometry assay kit (BD Biosciences, Cat#556547) was employed to assess cell death in H357-S/R and H357-R *POLK* KO cells. Cells were harvested 48 hours post-treatment via trypsinization. Following the manufacturer's guidelines, the cells were stained with annexin V and Propidium Iodide (PI) after a single wash with 1X PBS. In brief, 100  $\mu$ l of 1X annexin V binding buffer was added to the cells, which were subsequently incubated in the dark for 15 minutes with

FITC-conjugated annexin V to assess phosphatidylserine translocation, alongside Propidium iodide (PI) to evaluate membrane integrity. Ultimately, each reaction was adjusted with 400  $\mu$ l of 1X annexin V binding buffer just before the flow cytometry analysis (BD LSR Fortessa). The quantification of apoptosis percentages was examined using FlowJo V.10 software.

## Immunofluorescence staining

Cells were seeded at 70% confluency on glass coverslips under standard cell culture conditions and allowed to attach for 24 hours. First, cells were fixed using 4% formaldehyde for 15 minutes and subsequently permeabilized with 0.2% Triton X-100 in PBS for 10 minutes. Cells were subsequently blocked using 10% FBS in 1X PBS with 0.2% Triton-X-100 for a duration of 45 minutes to 1 hour at 37°C. The fixed cells were incubated overnight with primary antibodies (1:200-400 dilution) like Polk, phospho-Histone H2A.X (Ser139), Ki-67, p12, p50, Pol $\theta$ , USP2 and USP18. Following three washes with 1X PBS, the coverslips were incubated with secondary antibodies anti-mouse IgG Alexa Fluor 488 (Invitrogen, Cat#A-11017), anti-rabbit IgG Alexa Fluor 594 (Invitrogen, Cat#A-21207) and anti-rat IgG Alexa Fluor 555 (Invitrogen, Cat#A-21434) with 1:500 dilution for 1 hour. The coverslips were further washed, stained with DAPI, and mounted. Images were obtained using a confocal laser scanning microscope (Stellaris 5, Leica, Germany). The foci were quantified using ImageJ software. The co-localization percentage and scatter plot were obtained from Stellaris 5. The percentage of Ki-67 positive cells was calculated as: (number of positive cells in a field/total number of cells in a field) X 100.

## Alkaline comet assay

Cells were seeded in 6-well plates and treated with cisplatin (5  $\mu$ M) for 48 hours. Both control (i.e. without treatment) and cisplatin-treated cells were trypsinized and collected. The cells were then mixed with 0.5% low-melting agarose (LMA, cat#1613111) and fixed onto slides pre-coated with 1.5% agarose. Lysis was carried out in 20-30 ml of lysis buffer (2.5 M NaCl, 0.1 M EDTA, 10 mM Tris-HCl; pH=10) for 1 hour at 4°C in the dark, followed by neutralization with a buffer (300 mM NaOH, 1 mM EDTA; pH>13) for 20 mins at 4°C. Electrophoresis was performed in the alkaline buffer for 30 mins at 20V, after which the slides were dried and stained with Sytox green. Images were captured using an Apotome microscope (Zeiss). Data analysis was performed using Open-Comet software.

## MTT cell viability assay

The colorimetric-based cell viability assay using 3-(4,5-dimethylthiazol-2-yl)-2,5-diphenyl tetrazolium bromide (MTT) was carried out in 96-well microplates. Cells ( $5 \times 10^3$ ) were seeded in each well of 96-well plate and then treated with indicated concentrations of cisplatin and T2AA for 48 hours, and HU, aphidicolin and camptothecin for 24 hours. After treatment, media was removed and MTT (0.5 mg/ml) in PBS solution was added directly into wells and incubated for 3 hours. The medium was subsequently removed, and solvent (DMSO) was added to the cells to solubilize formazan crystals. The absorbance was measured at a wavelength of 570 nm after 20 minutes of shaking using a Multimode plate Reader (PerkinElmer).

## Cell cycle synchronization and cell cycle analysis

To arrest H357-S, H357-R and H357-R *POLK* KO cells in G1/S phase, cells were seeded into 10 cm<sup>2</sup> cell culture plates (corning) at a confluency of 30-40% in complete growth media and then allowed to grow overnight at 37°C with 5% CO<sub>2</sub>. The next day, cells were subjected to 2 mM thymidine in complete media for 12 hours (initial synchronization). Then cells were washed three times with 3 ml of 1X PBS and grown in a thymidine-free medium (first synchronization release) for 15 hours, then washed again three times with PBS and re-cultured in 2 mM thymidine containing complete growth media (second synchronization) for another 12 hours. Finally, cells were washed three times using 3 ml of 1X PBS and released from the G1/S arrest. Cells were taken at periods 0, 3, 6, 9, and 12 hours. For cisplatin treated sets; cisplatin was added to media during second synchronization release and cells were collected at mentioned intervals for cell cycle analyses. In

brief, the cells were collected via trypsinization and then washed two times with 2 ml of ice cold 1X PBS. Then fixed in chilled 70% ethanol. After washing with 1X PBS, the cells were resuspended in a buffer containing 0.2% Triton X-100, 50 µg/ml propidium iodide (PI), and 100 µg/ml RNase A, and incubated for 30 minutes in the dark. The data were recorded with a minimum of 10000 events using a BD LSR Fortessa machine and examined using FlowJo V.10 software.

## DNA fiber assay

A standardized protocol for the DNA fiber assay to follow the replication fork movement was followed. Briefly, cells were seeded for 24 hours prior to the start of the experiment. Then, cells were pulse-labeled with 30 µM CldU (Sigma, Cat#C6891) and 300 µM IdU (Sigma, Cat#I7125). For cisplatin-treated sets, cells were exposed to 5 µM of cisplatin for 24 hours before the addition of CldU and IdU. In the HU treatment set, cells were exposed to 2 mM hydroxyurea for 2 hours in-between two pulses. Cells were collected and resuspended in ice-cold PBS at a density of  $2.5 \times 10^5$  cells/ml. Labelled cells were then mixed with unlabelled cells at a 1:1 ratio. Subsequently, 2.5 µl of the cell suspension was placed onto a clean Superfrost plus microscope glass slide (Fisher Scientific, Cat#1255015). Cells were treated with 7.5 µl of lysis solution (200 mM Tris-HCl; pH 7.4, 50 mM EDTA, 0.5% SDS) and lysed by slight swirling by 10 µl micropipette tip; then pipetting the mixture up and down. The slides were kept in parallel position for 8-10 minutes for lysis, after which they were tilted to 45° to facilitate fiber spreading and allowed to air-dry for approximately 30 minutes. The samples were fixed in methanol and acetic acid solution (3:1) overnight at 4°C, washed twice with 1X PBS the following day, and then denatured with hydrochloric acid (2.5 N) for 1 hour. Subsequently, slides were incubated in a blocking solution (2% BSA, 0.1% Tween-20 in 1X PBS, sterile filtered) and stained with anti-rat CldU antibody (1:200, AbCam, Cat#ab6326) and anti-mouse IdU antibody (1:100, BD Biosciences, Cat#347580) for 2.5 hours. Then the slides were subjected to five washes with PBS-T (0.2% Tween-20) for three minutes each. Subsequently, they are briefly incubated with a blocking solution (2% BSA, 0.1% Tween-20, and 1X PBS). Slides were treated with anti-mouse Alexa Fluor 488 (Invitrogen, Cat#A11001) and anti-rat antibody (Jackson ImmunoResearch, Cat#712-166-153). Following secondary antibody staining, the slides were washed with PBS-T five times for three minutes each. The slides were thoroughly air-dried and mounted using Fluoromount aqueous mounting media (Sigma, Cat#F4680), with coverslips sealed with clear nail polish. Slides were captured at 63X magnification using Stellaris5 (Leica, Germany), and fiber length was assessed using ImageJ software, and fork speed was calculated using the following formula: Average length of (IdU+CldU) per 30 mins (i.e., Time of pulse).

## Quantification and statistical analyses

Data were represented as mean  $\pm$  SEM. Statistical analyses were performed using GraphPad Prism 9.0.0, and p values < 0.05 were considered statistically significant.

## Data availability

Data sharing is not applicable to the paper.

## Acknowledgements

We thank Mr. Sitendra Prasad Panda, Mr. Bhabani Shankar Sahoo, and Mr. Paritosh Nath for their technical assistance in the laboratory, Imaging facility and FACS facility, respectively. Our laboratory colleagues are acknowledged for their thoughtful discussion. JKS and IS are CSIR-Senior Research Fellows, and ST is thankful to DBT-RA fellowship.

## Additional information

### Authors' contributions

Ipsita Subhadarsini: Writing – original draft, Validation, Investigation, Formal analysis, Data curation, Resources, Methodology, and Writing—review and editing; Jugal Kishor Sahu: Writing – original draft, Validation, Investigation, Formal analysis, Data curation, Resources, Methodology, and Writing—review and editing; Shweta Thakur: Writing – original draft, Validation, Investigation, Formal analysis, Data curation, Resources, Methodology, and Writing—review and editing; Rupesh Dash: Resources, Supervision, and Writing—review and editing; Narottam Acharya: Writing – original draft, Formal analysis, Conceptualization, Supervision, Funding acquisition, Project administration, and Writing—review and editing

### Abbreviations

TLS: Translesion Synthesis  
Pol: DNA polymerase  
Pol?: DNA polymerase delta  
PCNA: Proliferating cell nuclear antigen  
DDR: DNA damage response  
PIP: PCNA interacting protein  
NER: Nucleotide excision repair  
DSBs: Double strand breaks  
HR: Homologous recombination  
NHEJ: Non-homologous end joining  
OSCC: oral squamous cell carcinoma  
HU: hydroxyurea

### Funding

Funder	Grant reference number	Author
Institute of Life Sciences		Narottam Acharya

### Author ORCID iDs

**Narottam Acharya:**  <https://orcid.org/0000-0001-8858-5418>

## Additional files

[Supplementary File 1.](#) 

[Supplementary File 2.](#) 

## References

1. Acharya N, Khandagale P, Thakur S, Sahu JK, Utkalaja BG (2020a) Quaternary structural diversity in eukaryotic DNA polymerases: monomeric to multimeric form. *Current genetics* **66**:635-655 <https://doi.org/10.1007/s00294-020-01071-1> | PubMed
2. Acharya N, Patel SK, Sahu SR, Kumari P (2020b) 'PIPs' in DNA polymerase: PCNA interaction affairs. *Biochemical Society transactions* **48**:2811-2822 <https://doi.org/10.1042/bst20200678> | PubMed
3. Alonso-de Vega I, Martin Y, Smits VA (2014) USP7 controls Chk1 protein stability by direct deubiquitination. *Cell cycle* **13**:3921-3926 <https://doi.org/10.4161/15384101.2014.973324> | PubMed
4. Bahassi EM, Ovesen JL, Riesenber AL, Bernstein WZ, Hasty PE, Stambrook PJ (2008) The checkpoint kinases Chk1 and Chk2 regulate the functional associations between hBRCA2 and Rad51 in response to DNA damage. *Oncogene* **27**:3977-3985 <https://doi.org/10.1038/onc.2008.17> | PubMed

5. Barnes RP, Hile SE, Lee MY, Eckert KA (2017) DNA polymerases eta and kappa exchange with the polymerase delta holoenzyme to complete common fragile site synthesis. *DNA repair* **57**:1-11 <https://doi.org/10.1016/j.dnarep.2017.05.006> | PubMed
6. Baynton K, Bresson-Roy A, Fuchs RP (1998) Analysis of damage tolerance pathways in *Saccharomyces cerevisiae*: a requirement for Rev3 DNA polymerase in translesion synthesis. *Molecular and cellular biology* **18**:960-966 <https://doi.org/10.1128/mcb.18.2.960> | PubMed
7. Bohgaki M, Hakem A, Halaby MJ, Bohgaki T, Li Q, Bissey PA, Shloush J, Kislinger T, Sanchez O, Sheng Y, et al. (2013) The E3 ligase PIRH2 polyubiquitylates CHK2 and regulates its turnover. *Cell Death Differ* **20**:812-822 <https://doi.org/10.1038/cdd.2013.7> | PubMed
8. Borsos BN, Majoros H, Pankotai T (2020) Ubiquitylation-Mediated Fine-Tuning of DNA Double-Strand Break Repair. *Cancers* **12** <https://doi.org/10.3390/cancers12061617> | PubMed
9. Casper AM, Nghiem P, Arlt MF, Glover TW (2002) ATR regulates fragile site stability. *Cell* **111**:779-789 [https://doi.org/10.1016/s0092-8674\(02\)01113-3](https://doi.org/10.1016/s0092-8674(02)01113-3) | PubMed
10. Cassidy KB, Bang S, Kurokawa M, Gerber SA (2020) Direct regulation of Chk1 protein stability by E3 ubiquitin ligase HUWE1. *The FEBS journal* **287**:1985-1999 <https://doi.org/10.1111/febs.15132> | PubMed
11. Chatterjee N, Whitman MA, Harris CA, Min SM, Jonas O, Lien EC, Luengo A, Vander Heiden MG, Hong J, Zhou P, et al. (2020) REV1 inhibitor JH-RE-06 enhances tumor cell response to chemotherapy by triggering senescence hallmarks. *Proceedings of the National Academy of Sciences of the United States of America* **117**:28918-28921 <https://doi.org/10.1073/pnas.2016064117> | PubMed
12. Chen Y, Zhao Y, Yang X, Ren X, Huang S, Gong S, Tan X, Li J, He S, Li Y, et al. (2022) USP44 regulates irradiation-induced DNA double-strand break repair and suppresses tumorigenesis in nasopharyngeal carcinoma. *Nature communications* **13**:501 <https://doi.org/10.1038/s41467-022-28158-2> | PubMed
13. Cheng YC, Shieh SY (2018) Deubiquitinating enzyme USP3 controls CHK1 chromatin association and activation. *Proceedings of the National Academy of Sciences of the United States of America* **115**:5546-5551 <https://doi.org/10.1073/pnas.1719856115> | PubMed
14. Chin TM, Quinlan MP, Singh A, Sequist LV, Lynch TJ, Haber DA, Sharma SV, Settleman J (2008) Reduced Erlotinib sensitivity of epidermal growth factor receptor-mutant non-small cell lung cancer following cisplatin exposure: a cell culture model of second-line erlotinib treatment. *Clinical cancer research : an official journal of the American Association for Cancer Research* **14**:6867-6876 <https://doi.org/10.1158/1078-0432.ccr-08-0093> | PubMed
15. Ciccia A, Elledge SJ (2010) The DNA damage response: making it safe to play with knives. *Molecular cell* **40**:179-204 <https://doi.org/10.1016/j.molcel.2010.09.019> | PubMed
16. D'Andrea A, Pellman D (1998) Deubiquitinating enzymes: a new class of biological regulators. *Critical reviews in biochemistry and molecular biology* **33**:337-352 <https://doi.org/10.1080/10409239891204251> | PubMed
17. Dall'Osto M, Pierini L, Valery N, Hoffmann JS, Pillaire MJ (2021) A Catalytically Independent Function of Human DNA Polymerase Kappa Controls the Stability and Abundance of Checkpoint Kinase 1. *Molecular and cellular biology* **41**:e0009021 <https://doi.org/10.1128/mcb.00090-21> | PubMed
18. Dasari S, Tchounwou PB (2014) Cisplatin in cancer therapy: molecular mechanisms of action. *European journal of pharmacology* **740**:364-378 <https://doi.org/10.1016/j.ejphar.2014.07.025> | PubMed
19. Dash RC, Ozen Z, Rizzo AA, Lim S, Korzhnev DM, Hadden MK (2018) Structural Approach To Identify a Lead Scaffold That Targets the Translesion Synthesis Polymerase Rev1. *Journal of chemical information and modeling* **58**:2266-2277 <https://doi.org/10.1021/acs.jcim.8b00535> | PubMed
20. Davis MI, Pragani R, Fox JT, Shen M, Parmar K, Gaudiano EF, Liu L, Tanega C, McGee L, Hall MD, et al. (2016) Small Molecule Inhibition of the Ubiquitin-specific Protease USP2 Accelerates cyclin D1 Degradation and Leads to Cell Cycle Arrest in Colorectal Cancer and Mantle Cell Lymphoma Models.

- The Journal of biological chemistry* **291**:24628-24640 <https://doi.org/10.1074/jbc.m116.738567> | PubMed
21. Doles J, Oliver TG, Cameron ER, Hsu G, Jacks T, Walker GC, Hemann MT (2010) Suppression of Rev3, the catalytic subunit of Pol{zeta}, sensitizes drug-resistant lung tumors to chemotherapy. *Proceedings of the National Academy of Sciences of the United States of America* **107**:20786-20791 <https://doi.org/10.1073/pnas.1011409107> | PubMed
  22. Duan M, Ulibarri J, Liu KJ, Mao P (2020) Role of Nucleotide Excision Repair in Cisplatin Resistance. *International journal of molecular sciences* **21** <https://doi.org/10.3390/ijms21239248> | PubMed
  23. Forment JV, Blasius M, Guerini I, Jackson SP (2011) Structure-specific DNA endonuclease Mus81/Eme1 generates DNA damage caused by Chk1 inactivation. *PLoS one* **6**:e23517 <https://doi.org/10.1371/journal.pone.0023517> | PubMed
  24. Garcia-Limones C, Lara-Chica M, Jimenez-Jimenez C, Perez M, Moreno P, Munoz E, Calzado MA (2016) CHK2 stability is regulated by the E3 ubiquitin ligase SIAH2. *Oncogene* **35**:4289-4301 <https://doi.org/10.1038/onc.2015.495> | PubMed
  25. Geng L, Liu F, Yang L, Liu Y, Wu G (2024) USP18 promotes the proliferation, invasion, and migration of head and neck squamous cell carcinoma by deubiquitinating PLK1. *Experimental cell research* **442**:114284 <https://doi.org/10.1016/j.yexcr.2024.114284> | PubMed
  26. Ghosh S (2019) Cisplatin: The first metal based anticancer drug. *Bioorg Chem* **88**:102925 <https://doi.org/10.1016/j.bioorg.2019.102925> | PubMed
  27. Gonzalez Besteiro MA, Gottifredi V (2015) The fork and the kinase: a DNA replication tale from a CHK1 perspective. *Mutat Res Rev Mutat Res* **763**:168-180 <https://doi.org/10.1016/j.mrrev.2014.10.003> | PubMed
  28. Gottifredi V, Karni-Schmidt O, Shieh SS, Prives C (2001) p53 down-regulates CHK1 through p21 and the retinoblastoma protein. *Molecular and cellular biology* **21**:1066-1076 <https://doi.org/10.1128/mcb.21.4.1066-1076.2001> | PubMed
  29. Guervilly JH, Renaud E, Takata M, Rosselli F (2011) USP1 deubiquitinase maintains phosphorylated CHK1 by limiting its DDB1-dependent degradation. *Human molecular genetics* **20**:2171-2181 <https://doi.org/10.1093/hmg/ddr103> | PubMed
  30. Hakura A, Sui H, Sonoda J, Matsuda T, Nohmi T (2019) DNA polymerase kappa counteracts inflammation-induced mutagenesis in multiple organs of mice. *Environmental and molecular mutagenesis* **60**:320-330 <https://doi.org/10.1002/em.22272> | PubMed
  31. Haracska L, Prakash L, Prakash S (2002) Role of human DNA polymerase kappa as an extender in translesion synthesis. *Proceedings of the National Academy of Sciences of the United States of America* **99**:16000-16005 <https://doi.org/10.1073/pnas.252524999> | PubMed
  32. Hirao A, Cheung A, Duncan G, Girard PM, Elia AJ, Wakeham A, Okada H, Sarkissian T, Wong JA, Sakai T, et al. (2002) Chk2 is a tumor suppressor that regulates apoptosis in both an ataxia telangiectasia mutated (ATM)-dependent and an ATM-independent manner. *Molecular and cellular biology* **22**:6521-6532 <https://doi.org/10.1128/mcb.22.18.6521-6532.2002> | PubMed
  33. Honke N, Shaabani N, Zhang DE, Hardt C, Lang KS (2016) Multiple functions of USP18. *Cell death & disease* **7**:e2444 <https://doi.org/10.1038/cddis.2016.326> | PubMed
  34. Jha V, Ling H (2018) Structural Basis for Human DNA Polymerase Kappa to Bypass Cisplatin Intrastrand Cross-Link (Pt-GG) Lesion as an Efficient and Accurate Extender. *Journal of molecular biology* **430**:1577-1589 <https://doi.org/10.1016/j.jmb.2018.04.023> | PubMed
  35. Kanemaru Y, Suzuki T, Niimi N, Gruz P, Matsumoto K, Adachi N, Honma M, Nohmi T (2015) Catalytic and non-catalytic roles of DNA polymerase kappa in the protection of human cells against genotoxic stresses. *Environmental and molecular mutagenesis* **56**:650-662 <https://doi.org/10.1002/em.21961> | PubMed

36. **Khandagale P**, Peroumal D, Manohar K, Acharya N (2019) Human DNA polymerase delta is a pentameric holoenzyme with a dimeric p12 subunit. *Life Sci Alliance* **2** <https://doi.org/10.26508/lsa.201900323> | PubMed
37. **Kim H**, Kim D, Choi H, Shin G, Lee JK (2023) Deubiquitinase USP2 stabilizes the MRE11-RAD50-NBS1 complex at DNA double-strand break sites by counteracting the ubiquitination of NBS1. *The Journal of biological chemistry* **299**:102752 <https://doi.org/10.1016/j.jbc.2022.102752> | PubMed
38. **Korzhev DM**, Hadden MK (2016) Targeting the Translesion Synthesis Pathway for the Development of Anti-Cancer Chemotherapeutics. *Journal of medicinal chemistry* **59**:9321-9336 <https://doi.org/10.1021/acs.jmedchem.6b00596> | PubMed
39. **Kumari N**, Kaur E, Raghavan SC, Sengupta S (2025) Regulation of pathway choice in DNA repair after double-strand breaks. *Curr Opin Pharmacol* **80**:102496 <https://doi.org/10.1016/j.coph.2024.102496> | PubMed
40. **Li T**, Huang X, Xu W, Qi J, Liu L, Chen P, Cao Y (2026) USP2 Promotes Nasopharyngeal Carcinoma Progression by Activating TRAF2/NF-kappaB Signaling and Stabilizing MMP2. *Molecular carcinogenesis* **65**:94-105 <https://doi.org/10.1002/mc.70054> | PubMed
41. **Lin X**, Okuda T, Trang J, Howell SB (2006) Human REV1 modulates the cytotoxicity and mutagenicity of cisplatin in human ovarian carcinoma cells. *Molecular pharmacology* **69**:1748-1754 <https://doi.org/10.1124/mol.105.020446> | PubMed
42. **Liu J**, Cao L, Wang Y, Zou Y, Guo Q, Chen S, Jiang B, Wu X, Zheng L, Zhang S, *et al.* (2024) The phosphorylation-deubiquitination positive feedback loop of the CHK2-USP7 axis stabilizes p53 under oxidative stress. *Cell reports* **43**:114366 <https://doi.org/10.1016/j.celrep.2024.114366> | PubMed
43. **Lovly CM**, Yan L, Ryan CE, Takada S, Piwnicka-Worms H (2008) Regulation of Chk2 ubiquitination and signaling through autophosphorylation of serine 379. *Molecular and cellular biology* **28**:5874-5885 <https://doi.org/10.1128/mcb.00821-08> | PubMed
44. **Mah LJ**, El-Osta A, Karagiannis TC (2010) gammaH2AX: a sensitive molecular marker of DNA damage and repair. *Leukemia* **24**:679-686 <https://doi.org/10.1038/leu.2010.6> | PubMed
45. **Maji S**, Panda S, Samal SK, Shriwas O, Rath R, Pellecchia M, Emdad L, Das SK, Fisher PB, Dash R (2018) Bcl-2 Antiapoptotic Family Proteins and Chemoresistance in Cancer. *Adv Cancer Res* **137**:37-75 <https://doi.org/10.1016/bs.acr.2017.11.001> | PubMed
46. **Maji S**, Shriwas O, Samal SK, Priyadarshini M, Rath R, Panda S, Das Majumdar SK, Muduly DK, Dash R (2019) STAT3- and GSK3beta-mediated Mcl-1 regulation modulates TPF resistance in oral squamous cell carcinoma. *Carcinogenesis* **40**:173-183 <https://doi.org/10.1093/carcin/bgy135> | PubMed
47. **Manohar K**, Peroumal D, Acharya N (2018) TLS dependent and independent functions of DNA polymerase eta (Poleta/Rad30) from Pathogenic Yeast *Candida albicans*. *Molecular microbiology* **110**:707-727 <https://doi.org/10.1111/mmi.14004> | PubMed
48. **Masters JR**, Koberle B (2003) Curing metastatic cancer: lessons from testicular germ-cell tumours. *Nat Rev Cancer* **3**:517-525 <https://doi.org/10.1038/nrc1120> | PubMed
49. **Messick TE**, Greenberg RA (2009) The ubiquitin landscape at DNA double-strand breaks. *The Journal of cell biology* **187**:319-326 <https://doi.org/10.1083/jcb.200908074> | PubMed
50. **Mohapatra P**, Shriwas O, Mohanty S, Ghosh A, Smita S, Kaushik SR, Arya R, Rath R, Das Majumdar SK, Muduly DK, *et al.* (2021) CMTM6 drives cisplatin resistance by regulating Wnt signaling through the ENO-1/AKT/GSK3beta axis. *JCI Insight* **6** <https://doi.org/10.1172/jci.insight.143643> | PubMed
51. **Oerlemans R**, Franke NE, Assaraf YG, Cloos J, van Zantwijk I, Berkers CR, Scheffer GL, Debipersad K, Vojtekova K, Lemos C, *et al.* (2008) Molecular basis of bortezomib resistance: proteasome subunit beta5 (PSMB5) gene mutation and overexpression of PSMB5 protein. *Blood* **112**:2489-2499 <https://doi.org/10.1182/blood-2007-08-104950> | PubMed
52. **Ogi T**, Shinkai Y, Tanaka K, Ohmori H (2002) Polkappa protects mammalian cells against the lethal and mutagenic effects of benzo[a]pyrene. *Proceedings of the National Academy of Sciences of the United States of America* **99**:15548-15553 <https://doi.org/10.1073/pnas.222377899> | PubMed

53. Ohashi E, Ogi T, Kusumoto R, Iwai S, Masutani C, Hanaoka F, Ohmori H (2000) Error-prone bypass of certain DNA lesions by the human DNA polymerase kappa. *Genes & development* **14**:1589-1594 <https://doi.org/10.1101/gad.14.13.1589> | PubMed
54. Patel SM, Dash RC, Hadden MK (2021) Translesion synthesis inhibitors as a new class of cancer chemotherapeutics. *Expert Opin Investig Drugs* **30**:13-24 <https://doi.org/10.1080/13543784.2021.1850692> | PubMed
55. Peng C, Chen Z, Wang S, Wang HW, Qiu W, Zhao L, Xu R, Luo H, Chen Y, Chen D, *et al.* (2016) The Error-Prone DNA Polymerase kappa Promotes Temozolomide Resistance in Glioblastoma through Rad17-Dependent Activation of ATR-Chk1 Signaling. *Cancer research* **76**:2340-2353 <https://doi.org/10.1158/0008-5472.can-15-1884> | PubMed
56. Pillaire MJ, Betous R, Hoffmann JS (2014) Role of DNA polymerase kappa in the maintenance of genomic stability. *Mol Cell Oncol* **1**:e29902 <https://doi.org/10.4161/mco.29902> | PubMed
57. Sahu JK, Subhadarsini I, Thakur S, Acharya N (2026) Differential functions of human DNA polymerase delta with p12 variants during DNA replication and DNA damage response. *Molecular biology of the cell* **37**:ar29 <https://doi.org/10.1091/mbc.e25-12-0580> | PubMed
58. Sahu JK, Thakur S, Subhadarsini I, Acharya N (2024) p12 isoform-2 is a regulatory subunit of human DNA polymerase delta and is dysregulated in various cancers. *FEBS letters* **598**:3087-3104 <https://doi.org/10.1002/1873-3468.15070> | PubMed
59. Sarkar S, Davies AA, Ulrich HD, McHugh PJ (2006) DNA interstrand crosslink repair during G1 involves nucleotide excision repair and DNA polymerase zeta. *The EMBO journal* **25**:1285-1294 <https://doi.org/10.1038/sj.emboj.7600993> | PubMed
60. Saxena S, Dixit S, Somyajit K, Nagaraju G (2019) ATR Signaling Uncouples the Role of RAD51 Paralogs in Homologous Recombination and Replication Stress Response. *Cell reports* **29**:551-559. <https://doi.org/10.1016/j.celrep.2019.09.008> | PubMed
61. Selles-Baiget S, Ambjorn SM, Carli A, Hendriks IA, Gallina I, Davey NE, Benedict B, Zarantonello A, Gadi SA, Meeusen B, *et al.* (2025) Catalytic and noncatalytic functions of DNA polymerase kappa in translesion DNA synthesis. *Nature structural & molecular biology* **32**:300-314 <https://doi.org/10.1038/s41594-024-01395-3> | PubMed
62. Seo GJ, Kim SE, Lee YM, Lee JW, Lee JR, Hahn MJ, Kim ST (2003) Determination of substrate specificity and putative substrates of Chk2 kinase. *Biochemical and biophysical research communications* **304**:339-343 [https://doi.org/10.1016/s0006-291x\(03\)00589-8](https://doi.org/10.1016/s0006-291x(03)00589-8) | PubMed
63. Sharma A, Almasan A (2020) USP14 Regulates DNA Damage Response and Is a Target for Radiosensitization in Non-Small Cell Lung Cancer. *International journal of molecular sciences* **21** <https://doi.org/10.3390/ijms21176383> | PubMed
64. Sharma A, Alswillah T, Kapoor I, Debjani P, Willard B, Summers MK, Gong Z, Almasan A (2020) USP14 is a deubiquitinase for Ku70 and critical determinant of non-homologous end joining repair in autophagy and PTEN-deficient cells. *Nucleic acids research* **48**:736-747 <https://doi.org/10.1093/nar/gkz1103> | PubMed
65. Sharma S, Shah NA, Joiner AM, Roberts KH, Canman CE (2012) DNA polymerase zeta is a major determinant of resistance to platinum-based chemotherapeutic agents. *Molecular pharmacology* **81**:778-787 <https://doi.org/10.1124/mol.111.076828> | PubMed
66. Shriwas O, Arya R, Mohanty S, Mohapatra P, Kumar S, Rath R, Kaushik SR, Pahwa F, Murmu KC, Majumdar SKD, *et al.* (2021) RRB1 rewires cisplatin resistance in oral squamous cell carcinoma by regulating Hippo pathway. *British journal of cancer* **124**:2004-2016 <https://doi.org/10.1038/s41416-021-01336-7> | PubMed
67. Slyskova J, Sabatella M, Ribeiro-Silva C, Stok C, Theil AF, Vermeulen W, Lans H (2018) Base and nucleotide excision repair facilitate resolution of platinum drugs-induced transcription blockage. *Nucleic acids research* **46**:9537-9549 <https://doi.org/10.1093/nar/gky764> | PubMed

68. **Srivastava AK**, Han C, Zhao R, Cui T, Dai Y, Mao C, Zhao W, Zhang X, Yu J, Wang QE (2015) Enhanced expression of DNA polymerase eta contributes to cisplatin resistance of ovarian cancer stem cells. *Proceedings of the National Academy of Sciences of the United States of America* **112**:4411-4416 <https://doi.org/10.1073/pnas.1421365112> | PubMed
69. **Stancel JN**, McDaniel LD, Velasco S, Richardson J, Guo C, Friedberg EC (2009) Polk mutant mice have a spontaneous mutator phenotype. *DNA repair* **8**:1355-1362 <https://doi.org/10.1016/j.dnarep.2009.09.003> | PubMed
70. **Swanton C**, Bernard E, Abbosh C, Andre F, Auwerx J, Balmain A, Bar-Sagi D, Bernards R, Bullman S, DeGregori J, *et al.* (2024) Embracing cancer complexity: Hallmarks of systemic disease. *Cell* **187**:1589-1616 <https://doi.org/10.1016/j.cell.2024.02.009> | PubMed
71. **Tan Y**, Wang Z, Xu M, Li B, Huang Z, Qin S, Nice EC, Tang J, Huang C (2023) Oral squamous cell carcinomas: state of the field and emerging directions. *International journal of oral science* **15**:44 <https://doi.org/10.1038/s41368-023-00249-w> | PubMed
72. **Tang F**, Wang Y, Zhao T, Yuan J, Kellum AH, Wang Y (2024) DNA polymerase kappa participates in early S-phase DNA replication in human cells. *Proceedings of the National Academy of Sciences of the United States of America* **121**:e2405473121 <https://doi.org/10.1073/pnas.2405473121> | PubMed
73. **Tang J**, Wu Z, Wang X, Hou Y, Bai Y, Tian Y (2022) Hypoxia-Regulated lncRNA USP2-AS1 Drives Head and Neck Squamous Cell Carcinoma Progression. *Cells* **11** <https://doi.org/10.3390/cells11213407> | PubMed
74. **Tang M**, Li S, Chen J (2021) Ubiquitylation in DNA double-strand break repair. *DNA repair* **103**:103129 <https://doi.org/10.1016/j.dnarep.2021.103129> | PubMed
75. **Temprine K**, Campbell NR, Huang R, Langdon EM, Simon-Vermot T, Mehta K, Clapp A, Chipman M, White RM (2020) Regulation of the error-prone DNA polymerase Polkappa by oncogenic signaling and its contribution to drug resistance. *Science signaling* **13** <https://doi.org/10.1126/scisignal.aau1453> | PubMed
76. **Thompson R**, Montano R, Eastman A (2012) The Mre11 nuclease is critical for the sensitivity of cells to Chk1 inhibition. *PloS one* **7**:e44021 <https://doi.org/10.1371/journal.pone.0044021> | PubMed
77. **Tonzi P**, Yin Y, Lee CWT, Rothenberg E, Huang TT (2018) Translesion polymerase kappa-dependent DNA synthesis underlies replication fork recovery. *eLife* **7** <https://doi.org/10.7554/elife.41426> | PubMed
78. **Torres MC**, Rebok A, Sun D, Spratt TE (2024) Activity of DNA polymerase kappa across the genome in human fibroblasts. *Proceedings of the National Academy of Sciences of the United States of America* **121**:e2403130121 <https://doi.org/10.1073/pnas.2403130121> | PubMed
79. **Tu Y**, Liu H, Zhu X, Shen H, Ma X, Wang F, Huang M, Gong J, Li X, Wang Y, *et al.* (2017) Ataxin-3 promotes genome integrity by stabilizing Chk1. *Nucleic acids research* **45**:4532-4549 <https://doi.org/10.1093/nar/gkx095> | PubMed
80. **Ummat A**, Rechkoblit O, Jain R, Roy Choudhury J, Johnson RE, Silverstein TD, Buku A, Lone S, Prakash L, Prakash S, *et al.* (2012) Structural basis for cisplatin DNA damage tolerance by human polymerase eta during cancer chemotherapy. *Nature structural & molecular biology* **19**:628-632 <https://doi.org/10.1038/nsmb.2295> | PubMed
81. **Vasquez-Del Carpio R**, Silverstein TD, Lone S, Johnson RE, Prakash L, Prakash S, Aggarwal AK (2011) Role of human DNA polymerase kappa in extension opposite from a cis-syn thymine dimer. *Journal of molecular biology* **408**:252-261 <https://doi.org/10.1016/j.jmb.2011.02.042> | PubMed
82. **Welsh C**, Day R, McGurk C, Masters JR, Wood RD, Koberle B (2004) Reduced levels of XPA, ERCC1 and XPF DNA repair proteins in testis tumor cell lines. *International journal of cancer* **110**:352-361 <https://doi.org/10.1002/ijc.20134> | PubMed
83. **Wojtaszek JL**, Chatterjee N, Najeeb J, Ramos A, Lee M, Bian K, Xue JY, Fenton BA, Park H, Li D, *et al.* (2019) A Small Molecule Targeting Mutagenic Translesion Synthesis Improves Chemotherapy. *Cell* **178**:152-159. <https://doi.org/10.1016/j.cell.2019.05.028> | PubMed

84. Wolfe WT, Washington MT, Prakash L, Prakash S (2003) Human DNA polymerase kappa uses template-primer misalignment as a novel means for extending mispaired termini and for generating single-base deletions. *Genes & development* **17**:2191-2199 <https://doi.org/10.1101/gad.1108603> | PubMed
85. Wu D, Miao J, Hu J, Li F, Gao D, Chen H, Feng Y, Shen Y, He A (2021) PSMB7 Is a Key Gene Involved in the Development of Multiple Myeloma and Resistance to Bortezomib. *Front Oncol* **11**:684232 <https://doi.org/10.3389/fonc.2021.684232> | PubMed
86. Wu J, Chen Y, Geng G, Li L, Yin P, Nowsheen S, Li Y, Wu C, Liu J, Zhao F, et al. (2019) USP39 regulates DNA damage response and chemo-radiation resistance by deubiquitinating and stabilizing CHK2. *Cancer letters* **449**:114-124 <https://doi.org/10.1016/j.canlet.2019.02.015> | PubMed
87. Yoon JH, Acharya N, Park J, Basu D, Prakash S, Prakash L (2014) Identification of two functional PCNA-binding domains in human DNA polymerase kappa. *Genes to cells : devoted to molecular & cellular mechanisms* **19**:594-601 <https://doi.org/10.1111/gtc.12156> | PubMed
88. Yoon JH, Johnson RE, Prakash L, Prakash S (2021) Implications of inhibition of Rev1 interaction with Y family DNA polymerases for cisplatin chemotherapy. *Genes & development* **35**:1256-1270 <https://doi.org/10.1101/gad.348662.121> | PubMed
89. Yoon JH, Park J, Conde J, Wakamiya M, Prakash L, Prakash S (2015) Rev1 promotes replication through UV lesions in conjunction with DNA polymerases eta, iota, and kappa but not DNA polymerase zeta. *Genes & development* **29**:2588-2602 <https://doi.org/10.1101/gad.272229.115> | PubMed
90. Zannini L, Delia D, Buscemi G (2014) CHK2 kinase in the DNA damage response and beyond. *Journal of molecular cell biology* **6**:442-457 <https://doi.org/10.1093/jmcb/mju045> | PubMed
91. Zhang M, Shao Y, Gu W (2023) The Mechanism of Ubiquitination or Deubiquitination Modifications in Regulating Solid Tumor Radiosensitivity. *Biomedicines* **11** <https://doi.org/10.3390/biomedicines11123240> | PubMed
92. Zhang YW, Brognard J, Coughlin C, You Z, Dolled-Filhart M, Aslanian A, Manning G, Abraham RT, Hunter T (2009) The F box protein Fbx6 regulates Chk1 stability and cellular sensitivity to replication stress. *Molecular cell* **35**:442-453 <https://doi.org/10.1016/j.molcel.2009.06.030> | PubMed
93. Zhang YW, Otterness DM, Chiang GG, Xie W, Liu YC, Mercurio F, Abraham RT (2005) Genotoxic stress targets human Chk1 for degradation by the ubiquitin-proteasome pathway. *Molecular cell* **19**:607-618 <https://doi.org/10.1016/j.molcel.2005.07.019> | PubMed
94. Zhao Y, Biertumpfel C, Gregory MT, Hua YJ, Hanaoka F, Yang W (2012) Structural basis of human DNA polymerase eta-mediated chemoresistance to cisplatin. *Proceedings of the National Academy of Sciences of the United States of America* **109**:7269-7274 <https://doi.org/10.1073/pnas.1202681109> | PubMed
95. Zhu L, Chen Z, Guo T, Chen W, Zhao L, Guo L, Pan X (2022) USP2 Inhibits Lung Cancer Pathogenesis by Reducing ARID2 Protein Degradation via Ubiquitination. *BioMed research international* **2022**:1525216 <https://doi.org/10.1155/2022/1525216> | PubMed
96. Zhu X, Zou S, Zhou J, Zhu H, Zhang S, Shang Z, Ding WQ, Wu J, Chen Y (2016) REV3L, the catalytic subunit of DNA polymerase zeta, is involved in the progression and chemoresistance of esophageal squamous cell carcinoma. *Oncology reports* **35**:1664-1670 <https://doi.org/10.3892/or.2016.4549> | PubMed

## Peer reviews

### Reviewer #1 (Public review):

Summary:

Cisplatin, a platinum-based chemotherapeutic agent, induces intra- and interstrand crosslinks, thereby blocking DNA replication and transcription and triggering apoptosis. The authors aim to demonstrate that DNA polymerase  $\kappa$  (Pol $\kappa$ ), traditionally seen as a translesion

synthesis (TLS) polymerase, able to synthesize DNA through DNA lesions, plays a non-catalytic, structural role in stabilizing replication forks and protecting cells from cisplatin-induced cytotoxicity. A key finding of this work is the identification of two novel molecular axes: PCNA-Pol $\kappa$ -Pol $\delta$ , which facilitates efficient DNA replication; PCNA-Pol $\kappa$ -USP18, which stabilizes DNA damage response proteins. These findings provide actionable therapeutic targets for overcoming head and neck squamous cell carcinoma chemoresistance, a cancer with rising incidence and limited treatment options.

#### Strengths:

The study relies on a robust experimental design, including Pol $\kappa$  allegedly CRISPR-Cas9 knockout, siRNA knockdown, and rescue experiments with wild-type, catalytically dead, and PCNA-interaction-deficient Pol $\kappa$  variants, supporting a non-catalytic role of Pol $\kappa$ . The work also reports a strong implication of Pol $\kappa$  in cisplatin resistance, the identification of USP18 as a possible Pol $\kappa$  partner and the consequences of Pol $\kappa$  depletion on post-translational stabilisation of DNA damage response proteins.

#### Weaknesses:

The findings reported in this manuscript cannot be generalized to all cisplatin resistance mechanisms, as cells may develop multiple adaptive strategies to survive chemotherapy. Pol $\kappa$ 's role varies across cancer types. For example, it is downregulated in stomach and colorectal cancers but upregulated in HNSCC, lung, and ovarian cancers. Thus, its use as a biomarker or drug target may be context-dependent.

Acute cisplatin exposure is sufficient to trigger Pol $\kappa$  upregulation to levels similar to those in resistant cells. However, it remains unclear how long this upregulation persists and to what extent it contributes to survival. Further, the sensitivity of cisplatin-naïve H357 or SCC9 cells (H357-S and SCC9-S) to Pol $\kappa$  knockdown has not been addressed. This is a critical question, as acute cisplatin exposure induces Pol $\kappa$  expression to levels similar to those in resistant cells. This could argue against a direct role for Pol $\kappa$  in mediating resistance and instead suggest indirect mechanisms (like Pol $\kappa$ -dependent mutations during adaptation).

The experimental design and results aimed at demonstrating the existence of a PCNA-Pol $\kappa$ -USP18 axis (Figure 9A) do not fully support the conclusion that these proteins form a stable complex. This set of experiments also lacks essential controls, such as the immunoprecipitated bait and the amount of immunoglobulins precipitated in all conditions. This also applies to the colocalization experiments in cells shown in Figure 9B. Images are poor and lack quantification. Further, Pol $\kappa$  is seen mainly cytoplasmic in the upper panel, while it is nuclear in the lower panel. Discrepancies in Pol $\kappa$  subcellular localization are also evident in the Supplementary data. USP18 is known to deubiquitinate ISG15-modified proteins (not just ubiquitin). The study does not rule out ISGylation as a contributing mechanism. The experimental design involving analysis of DNA synthesis dynamics at a single-molecule level is not appropriate. Overinterpretation of the data in several parts of the manuscript and lack of rigor in performing the experiments. Inappropriate consideration and absence of discussion of previously published literature directly related to the subject studied in this manuscript. Discrepancy with a previous report regarding the role of Pol $\kappa$  in Chk1 phosphorylation (Tonzi et al., eLife 2018). Synergic effect of T2AA inhibitor and Cisplatin have been already described in « naïve » cancer cells (Inoue et al, 2014). Another critical point is that the proliferation rate of Pol $\kappa$ -depleted cells is slower than that of wild-type cells. Hence, the colony formation assay shown in Figure 2B can be misleading, since the observed differences can be interpreted only as a proliferation problem.

<https://doi.org/10.7554/eLife.112155.1.sa3>

## Reviewer #2 (Public review):

### Summary:

Building on earlier studies, the authors report a role for pol kappa in mediated cisplatin resistance. Their data on dispensability of pol kappa catalytic activity for cisplatin resistance is consistent with previous reports. They further demonstrate that the PIP box of pol kappa is critical for cisplatin response. Based on these observations, the study concludes that targeting pol kappa and PCNA interaction can be a viable approach to overcome cisplatin resistance.

### Strengths:

Indications that interaction between Pol kappa PIP box and PCNA can be targeted to overcome cisplatin resistance.

### Weaknesses:

(1) The study has used a model of cisplatin resistance and found that the phenotype is specifically reliant on upregulation of Pol kappa. They also observe that in this model of cisplatin resistance, there is rapid degradation of multiple repair proteins, including ATM, ATR, HR and NHEJ proteins upon knocking out Pol kappa. However, it is unclear how the resistant model was derived. Also, since the data and almost all experiments in this manuscript were performed with a single model of cisplatin resistance, the conclusions should be taken with caution.

(2) There are also inconsistencies in findings. Increased G2 arrest and no change in origin firing are being observed despite a significant reduction in Chk1 protein levels.

<https://doi.org/10.7554/eLife.112155.1.sa2>

## Reviewer #3 (Public review):

This manuscript investigates the role of PolK in cisplatin repair. While in general it is considered that polK is not involved in the repair of cisplatin-induced DNA damage, the authors show that in a very specific scenario, namely cisplatin-resistant head and neck cancer cells, loss of PolK causes cisplatin sensitization, implying a role in cisplatin repair by polK in these cells. It is also implied that these cells acquire cisplatin resistance by overexpressing polK, but this is not really investigated. The authors then go on to show that DNA replication in the presence of cisplatin is affected by the loss of polK in these cells and also identify USP18 as a potential polK interactor in these cells with a similar phenotype. They claim that polK and USP18 form a pathway that allows cisplatin tolerance in these cisplatin-resistant head and neck cancer cells. The findings are interesting and useful to the field; however, the manuscript, in its current form, has several issues. Most importantly, the mechanism of USP18 has not been investigated. In addition, the manuscript does not flow fluidly, and instead, various experiments are put together without a clear logic. Some of the claims are not substantiated by the data shown.

(1) The experiments in Figure 1 using a few cell lines from various types of cancers are not enough to conclude that polK expression is specifically induced by cisplatin in some types of cancers but not others. Since the focus of this study is head and neck cancer, the authors should show the expression of PolK after cisplatin treatment in more head and neck cancer cell lines, and not just the two investigated.

(2) It is unclear to me why the authors include H357-S in their experiments. If the idea is that these cells acquire resistance because they overexpress polK, then the authors should

investigate this by exogenously overexpressing PolK in H357-S cells and test if these cells are cisplatin resistant.

(3) In addition, the authors should create the polK knockout in H357-S cells as well and include it as a control in their experiments.

(4) Page 6, line 28: the comet assay does not measure DNA degradation, but rather DNA breaks.

(5) Figure 4B: How does the overexpression of PolK mutants compare to endogenous PolK expression? It is important to assess if this expression is similar or of much higher magnitude.

(6) Page 9, line 22: "For such a function, the catalytic domain of PolK becomes dispensable, whereas its interaction with PCNA is sufficient to drive efficient replication". I do not understand what data the authors used to make this claim. The interaction and colocalization studies should be performed with the PIP mutant. Similarly, this mutant should be used in the HU DNA fiber assays.

(7) It is unclear how USP18 acts. What are its substrates? Chk1/2, BRCA1, BRCA2? This needs to be investigated. The impact of PolK on this activity needs to be assessed as well (is PolK needed for USP18-mediated de-ubiquitination of these DSB proteins?). As it stands, the manuscript does not address the mechanism of USP18 in DNA repair, which is billed as the main finding of the paper.

(8) Do PolK and USP18 interact directly? Experiments using recombinant proteins would be useful to address this.

<https://doi.org/10.7554/eLife.112155.1.sa1>

## Author response:

### Reviewer #1 (Public review):

#### Summary:

*Cisplatin, a platinum-based chemotherapeutic agent, induces intra- and interstrand crosslinks, thereby blocking DNA replication and transcription and triggering apoptosis. The authors aim to demonstrate that DNA polymerase  $\kappa$  (Polk), traditionally seen as a translesion synthesis (TLS) polymerase, able to synthesize DNA through DNA lesions, plays a non-catalytic, structural role in stabilizing replication forks and protecting cells from cisplatin-induced cytotoxicity. A key finding of this work is the identification of two novel molecular axes: PCNA-Polk-Pol $\delta$ , which facilitates efficient DNA replication; PCNA-Polk-USP18, which stabilizes DNA damage response proteins. These findings provide actionable therapeutic targets for overcoming head and neck squamous cell carcinoma chemoresistance, a cancer with rising incidence and limited treatment options.*

#### Strengths:

*The study relies on a robust experimental design, including Polk allegedly CRISPR-Cas9 knockout, siRNA knockdown, and rescue experiments with wild-type, catalytically dead, and PCNA interaction-deficient Polk variants, supporting a non-catalytic role of Polk. The work also reports a strong implication of Polk in cisplatin resistance, the identification of USP18 as a possible Polk partner and the consequences of Polk depletion on post-translational stabilisation of DNA damage response proteins.*

Thank you so much for appreciating our efforts to demonstrate role of Polk mediated axes in cisplatin resistance in head and neck cancer cells.

*Weaknesses:*

*The findings reported in this manuscript cannot be generalized to all cisplatin resistance mechanisms, as cells may develop multiple adaptive strategies to survive chemotherapy. Polk's role varies across cancer types. For example, it is downregulated in stomach and colorectal cancers but upregulated in HNSCC, lung, and ovarian cancers. Thus, its use as a biomarker or drug target may be context-dependent.*

We completely agree with you, and the presented data only support Polk's role in HNSCC as demonstrated in both acute cisplatin exposure as well as the cisplatin-resistant HNSCC models. Other cell and cancer types may adopt different strategies for cisplatin resistance.

*Acute cisplatin exposure is sufficient to trigger Polk upregulation to levels similar to those in resistant cells. However, it remains unclear how long this upregulation persists and to what extent it contributes to survival. Further, the sensitivity of cisplatin-naïve H357 or SCC9 cells (H357-S and SCC9-S) to Polk knockdown has not been addressed. This is a critical question, as acute cisplatin exposure induces Polk expression to levels similar to those in resistant cells. This could argue against a direct role for Polk in mediating resistance and instead suggest indirect mechanisms (like Polk-dependent mutations during adaptation).*

Since H357-S and SCC9-S cells are highly sensitive to cisplatin, knocking down of Polk unlikely will alter the phenotype, as other TLS DNA polymerases like Polk and Polk play critical role in such lesion bypass. Since no other DNA polymerase was upregulated in these cells upon cisplatin exposure and in the cisplatin-resistant cells, it was intriguing to demonstrate a direct role of Polk in chemoresistance and that has been proven in this study. Since the catalytic activity of Polk is not required to induce chemoresistant in these cells, we strongly believe that Polk-dependent mutagenesis play minimal or no role in adapting cells to tolerate cisplatin. Nevertheless, we will knock down Polk in these cells and determine cisplatin sensitivity

*The experimental design and results aimed at demonstrating the existence of a PCNA-Polk-USP18 axis (Figure 9A) do not fully support the conclusion that these proteins form a stable complex. This set of experiments also lacks essential controls, such as the immunoprecipitated bait and the amount of immunoglobulins precipitated in all conditions. This also applies to the colocalization experiments in cells shown in Figure 9B. Images are poor and lack quantification. Further, Polk is seen mainly cytoplasmic in the upper panel, while it is nuclear in the lower panel. Discrepancies in Polk subcellular localization are also evident in the Supplementary data.*

We appreciate the Reviewer's critical and insightful comment. In our view, the interaction between Polk and USP18 is very specific as USP2 and IgG alone do not pull down Polk. Similarly, we also show that both Polk and USP18 interact with PCNA. We agree with the reviewer that the existence of a stable complex of PCNA-Polk-USP18 has not been fully demonstrated in the current version. We will perform additional experiments to strengthen our finding: a) Co-IP experiments with Polk PIP mutants (wild-type vs. mutant) should be performed to determine whether USP18 loses its ability to bind PCNA in the absence of Polk-PCNA interaction. b) Mapping the domain in Polk that is involved in USP18 binding and their Co-IP experiment. Additionally, high resolution co-localisation images including quantified data will be provided.

*USP18 is known to deubiquitinate ISG15-modified proteins (not just ubiquitin). The study does not rule out ISGylation as a contributing mechanism.*

We find the point raised by the reviewer is very intriguing, however, as it will require a significant amount of time and effort to demonstrate ISGylation of DDR proteins and deISGylation by UPS18, and the insight that we may gain is unlikely to add to the central theme of this paper, we will expand this in our subsequent related study. Thank you for the suggestion.

*The experimental design involving analysis of DNA synthesis dynamics at a single-molecule level is not appropriate. Over interpretation of the data in several parts of the manuscript and lack of rigor in performing the experiments. Inappropriate consideration and absence of discussion of previously published literature directly related to the subject studied in this manuscript. Discrepancy with a previous report regarding the role of Polk in Chk1 phosphorylation (Tonzi et al., eLife 2018). Synergic effect of T2AA inhibitor and Cisplatin have been already described in « naive » cancer cells (Inoue et al, 2014).*

Thank you very much for the suggestions. We will take care of the portions and modify as suggested. The necessary reference will be added as appropriate.

*Another critical point is that the proliferation rate of Polk-depleted cells is slower than that of wild-type cells. Hence, the colony formation assay shown in Figure 2B can be misleading, since the observed differences can be interpreted only as a proliferation problem.*

Thank you for pointing this out and we will modify the portion for better clarity.

**Reviewer #2 (Public review):**

*Summary:*

*Building on earlier studies, the authors report a role for pol kappa in mediated cisplatin resistance. Their data on dispensability of pol kappa catalytic activity for cisplatin resistance is consistent with previous reports. They further demonstrate that the PIP box of pol kappa is critical for cisplatin response. Based on these observations, the study concludes that targeting pol kappa and PCNA interaction can be a viable approach to overcome cisplatin resistance.*

*Strengths:*

*Indications that interaction between Pol kappa PIP box and PCNA can be targeted to overcome cisplatin resistance.*

Thank you for appreciating our finding that the PIP box of Polk is critical for cisplatin response

*Weaknesses:*

*(1) The study has used a model of cisplatin resistance and found that the phenotype is specifically reliant on upregulation of Pol kappa. They also observe that in this model of cisplatin resistance, there is rapid degradation of multiple repair proteins, including ATM, ATR, HR and NHEJ proteins upon knocking out Pol kappa. However, it is unclear how the resistant model was derived. Also, since the data and almost all experiments in this manuscript were performed with a single model of cisplatin resistance, the conclusions should be taken with caution.*

We are extremely sorry for the lack of clarity. Please note that two cisplatin-resistant models (H357 and SSC9) have been used and the results were very consistent in both cells. Fig. 1C

clearly demonstrates about the generation of these resistant models and the original reference has been already cited.

*(2) There are also inconsistencies in findings. Increased G2 arrest and no change in origin firing are being observed despite a significant reduction in Chk1 protein levels.*

Thank you for pointing this out. In our view, the increased G2 arrest is due to more fork stalling or collapsed than the new origin firing. Also, in our assay we observed less than 10% of new origin fired DNA fibres, and that could be the reason of no significant change in new origin firing among various cells.

**Reviewer #3 (Public review):**

*This manuscript investigates the role of PolK in cisplatin repair. While in general it is considered that polK is not involved in the repair of cisplatin-induced DNA damage, the authors show that in a very specific scenario, namely cisplatin-resistant head and neck cancer cells, loss of PolK causes cisplatin sensitization, implying a role in cisplatin repair by polK in these cells. It is also implied that these cells acquire cisplatin resistance by overexpressing polK, but this is not really investigated. The authors then go on to show that DNA replication in the presence of cisplatin is affected by the loss of polK in these cells and also identify USP18 as a potential polK interactor in these cells with a similar phenotype. They claim that polK and USP18 form a pathway that allows cisplatin tolerance in these cisplatin-resistant head and neck cancer cells. The findings are interesting and useful to the field; however, the manuscript, in its current form, has several issues. Most importantly, the mechanism of USP18 has not been investigated. In addition, the manuscript does not flow fluidly, and instead, various experiments are put together without a clear logic. Some of the claims are not substantiated by the data shown.*

Thank you very much for finding our study interesting and the pending concerns will be addressed as suggested.

*(1) The experiments in Figure 1 using a few cell lines from various types of cancers are not enough to conclude that polK expression is specifically induced by cisplatin in some types of cancers but not others. Since the focus of this study is head and neck cancer, the authors should show the expression of PolK after cisplatin treatment in more head and neck cancer cell lines, and not just the two investigated.*

In this study, we have explored eight different cell types (breast, brain, liver, head and neck, pancreatic, prostate, lungs, and kidney) to check the expression of Polk upon cisplatin exposure, and HNSCC cells only showed Polk up-regulation. Therefore, we went ahead for further demonstration of the role of Polk in cisplatin resistance in OSCC using four different cell models (H357-S, H357-R, SSC9-S, and SSC9-R). By adding more cell lines to study will unlikely change the central theme of the paper. Yes, by acquiring and analysing clinical samples from the cisplatin responder and non-responders would have strengthen our finding.

*(2) It is unclear to me why the authors include H357-S in their experiments. If the idea is that these cells acquire resistance because they overexpress polK, then the authors should investigate this by exogenously overexpressing PolK in H357-S cells and test if these cells are cisplatin resistant.*

It's an interesting point and we will check whether overexpression of Polk in H357-S cells could induce resistance to cisplatin and alters IC<sub>50</sub>. Thank you for the suggestion.

*(3) In addition, the authors should create the polK knockout in H357-S cells as well and include it as a control in their experiments.*

We appreciate your suggestion. As suggested by Reviewer #1 also, we will check the phenotype of Polk knockdown H357-S cells.

(4) Page 6, line 28: the comet assay does not measure DNA degradation, but rather DNA breaks.

Thank you for the suggestion, we will modify the text accordingly.

(5) Figure 4B: How does the overexpression of PolK mutants compare to endogenous PolK expression? It is important to assess if this expression is similar or of much higher magnitude.

Please note that GFP-Polk has been overexpressed in H357 Polk knockout cells to nullify the effect of endogenous Polk, otherwise we will not be able to test the role of various Polk mutants.

(6) Page 9, line 22: "For such a function, the catalytic domain of Polk becomes dispensable, whereas its interaction with PCNA is sufficient to drive efficient replication". I do not understand what data the authors used to make this claim. The interaction and colocalization studies should be performed with the PIP mutant. Similarly, this mutant should be used in the HU DNA fiber assays.

We are extremely sorry for the lack of clarity. The inference has been derived from two sets of experiments as shown in Fig. 4C and Fig. 4D (and is with HU).

(7) It is unclear how USP18 acts. What are its substrates? Chk1/2, BRCA1, BRCA2? This needs to be investigated. The impact of PolK on this activity needs to be assessed as well (is PolK needed for USP18-mediated de-ubiquitination of these DSB proteins?). As it stands, the manuscript does not address the mechanism of USP18 in DNA repair, which is billed as the main finding of the paper.

It has already been demonstrated in Fig. 9C where by knocking down USP18, the DDR proteins like Chk1, Chk2, CtIP, and Artemis can be recovered for ubiquitin-mediated proteasomal degradation. The same results are also obtained when its interacting partner Polk is deleted. In our view, the presented results have sufficiently demonstrated the role of Polk-Usp18 in the repair of cisplatin adducts through DDR proteins.

(8) Do PolK and USP18 interact directly? Experiments using recombinant proteins would be useful to address this.

We appreciate your suggestion. Since the Usp18 protein is not readily available, we will not be able to show; however, we believe the interaction is direct, and we will be able to map the binding site in Polk.

<https://doi.org/10.7554/eLife.112155.1.sa0>